Chapter 1

Introduction

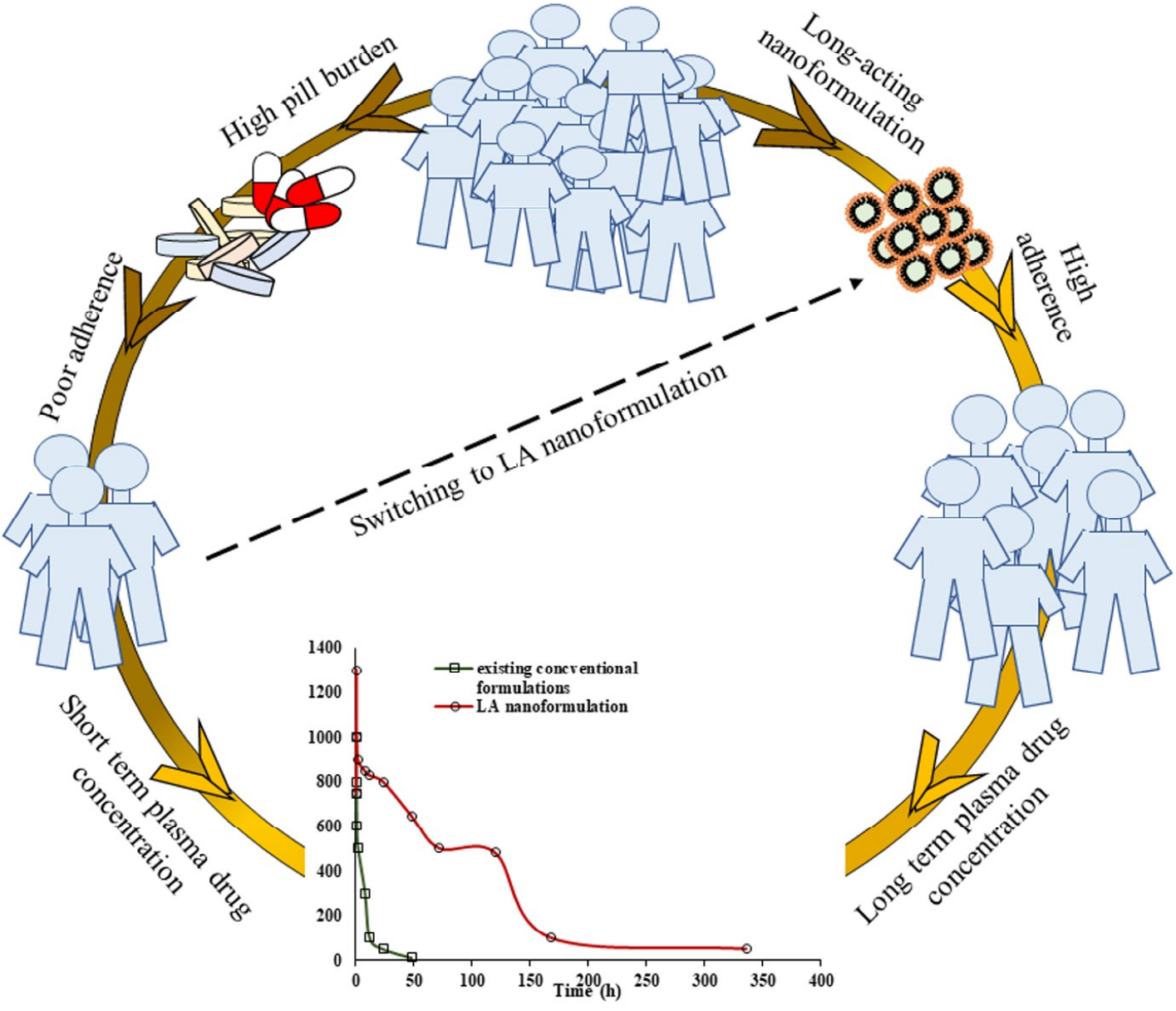

1. Background

Long-acting (LA) injectables have revolutionized the treatment measures for various diseases including schizophrenia, cancer, and asthma since 1990 [1]. It specifically holds significance for treatment and prophylaxis of diseases wherein; long term drug administration is essential [2]. Despite the existence of LA nanoformulations; their application for treatment and prophylaxis in infectious diseases including malaria, tuberculosis, and HIV is still at its inception. Perennial relapse of infectious diseases in humans and animals emanating from failure in treatment is a cause of solicitude for grave socio-economic loss [3,4]. Only recently one LA nanoformulation has been approved by Health Canada namely; Cabenuva™ by Jannsen Pharmaceutica (Beerse, Belgium) on 20th March, 2020 for once-monthly administration of cabotegravir and rilpivirine long-acting nanosuspension recommended for HIV-1 infected adults with suppressed and stable viral load [5]. However, the effect of various physicochemical properties of anti-infective drugs on drug loading, entrapment efficiency, primary (injection site) and secondary depot (immune cell) genesis and fundamental mechanism for long-acting potential of anti-infective nanoformulations remains unexplored.

With the advent of Cabenuva™, various nanoformulations including nanocrystals [6], nano-prodrug [7,8], solid drug nanoparticles [9], lipid [10–13] and polymeric nanoparticles [14,15] and nanosuspension [16,17] have been explored for LA antiretroviral (LA ARV) effect. While, only polymeric solid drug nanoparticles [18], nanocrystals [19,20], and polymeric nanoparticles [21] have been explored for LA anti-malarial and anti-tuberculosis effect. Therefore, current research aims in development, *in vitro,* and *in vivo* characterization of LA nanoformulations incorporating drugs with varied physicochemical properties against infectious diseases.

2. General considerations involved in the development of Long-acting nanoformulations

2.1 Desired physicochemical and pharmacokinetic properties of active pharmaceutical ingredients for Long-acting nanoformulations

The main objective of LA nanoformulations is to provide sustained drug release to achieve constant and effective plasma drug concentration at the desired site for weeks or months [22]. Orally administered drugs elicit decreased bioavailability due to hepatic first-pass metabolism and drug-drug interaction due to the presence of various transporters and metabolic enzymes in the intestinal epithelium, which can be avoided by LA nanoformulation [23]. Therefore, those physicochemical properties of the drugs, which determine stability, bioavailability, and efficacy of LA nanoformulations become vital [24,25]. In case, physicochemical properties of the orally administered drugs are not suitable for LA nanoformulation, new drug synthesis for LA effect is required [23]. Generally, orally administered active pharmaceutical ingredients (APIs) must satisfy the Lipinski rule of five. The rule states that those APIs which exhibit molecular weight, log P, hydrogen bond donors and acceptors must be <500 Da, <5, 5, and 10 respectively, are considered a good candidate for oral delivery [26–28]. The similar, rule could be extended to understand the properties of APIs suitable for LA nanoformulations. Further, other physicochemical properties including solubility and pK_a played a significant role in the design of LA nanoformulations. Those drugs which exhibit low aqueous solubility (<50 mg/ml), high log P (2-5), high potency with low therapeutic plasma drug concentration (<1000 ng/ml), and low pK_a are considered suitable for LA effect [23]. Higher pK_a of the drug leads to ionization at physiological pH below 7.4, causing increased drug solubility and electrostatic interaction between drug and excipients. Therefore, esterification of drugs to form prodrug with increased pKa leads to decreased dissolution of drug leading to longer half-life and increased potency [29]. For instance, cabotegravir was esterified to form myristoylated prodrug [7], emtricitabine converted to palmitoylated emtricitabine [30],

lamivudine and abacavir to phosphoramidate pronucleotide [31], rilpivirine to methyl tetradecanoate prodrug [8], and paliperidone to palmitate prodrug [32] to prepare LA nanoformulations. The pharmacokinetics of the drug depends upon the drug release from LA nanoformulation, solubility, molecular weight and log P. Therefore, for dual drug LA nanoformulation the pharmacokinetic of individual drug should be similar to avoid lack of effective plasma and site-specific concentration of either drug after certain time post-administration [11,24]. Further, the particle size of LA nanoformulations played a significant role in producing therapeutic effect for a longer duration. For instance, rilpivirine nanosuspension (200 nm) stabilized by poloxamer 338 depicted higher drug loading and sustained plasma concentration in humans compared with 400 nm and 800 nm vitamin E TPGS stabilized rilpivirine nanosuspension when injected by IM or SC, showed plasma concentration below 10 ng/ml after 3 or 6 months respectively. Further, the rilpivirine LA nanoformulation (200-600 mg dose) showed plasma concentration (73-95 ng/ml) above mean minimal concentration as obtained by daily once oral dosing. However, no difference was observed in plasma concentration after SC or IM route, ruling out the role of route of administration on LA potential of nanoformulation of different physicochemical properties in the same species [33]. Moreover, polarity of the drug also played a significant role in solubilization and absorption. It was observed that polar surface area (PSA) of 63°A elicited 90% oral bioavailability while only 10% oral bioavailability was exhibited for PSA of 139°A [34].

The suitability of the drug for LA nanoformulations should rather consider the Biopharmaceutical Drug Disposition Classification System (BDDS) wherein, class I and II consist of high solubility/extensively metabolized and low solubility/extensively metabolized API respectively. In contrast, class III and IV include high solubility/poorly metabolized and low solubility/poorly metabolized API [35]. The BDDS classification for drugs was an

extension to Biopharmaceutical Classification System (BCS) after observing the drug disposition mechanics in each class to predict drug absorption as well as disposition. The BDDS classification categorizes drugs into four groups wherein class I and II drugs lead to metabolic disposition in contrast to class III and IV which were eliminated by urine or bile. Drugs belonging to BDDS class II are the substrate for P-glycoprotein efflux, class III drugs are subjected to absorptive transporter effect while class IV are susceptible to efflux and absorptive transporter [36]. Thus, BDDS classification determines the transporter, enzymatic substrate, and drug-drug interaction in the liver, intestine, kidney, and brain. Generally, class II and IV drugs are suitable for lipid-based nanoformulations wherein transporter modifying carriers could be used. Moreover, both class II and IV drugs lead to a significant reduction in dose with >70% and <30% metabolism, respectively [36]; making these candidates suitable for LA nanoformulation. Further, poorly metabolized drugs exhibit sustained drug release potential due to low clearance. Therefore, proper *in-vitro in-vivo* correlation needs to be established along with an estimation of site-specific concentration and toxicity profile of BDDS class IV drug, if incorporated into LA nanoformulation [37]. Effective delivery of long-acting nanoformulations requires lower dose volume for administration. Therefore, those drugs which exhibit short half-life and high dose serve as poor candidates for LA nanoformulation, probably due to the requirement of high injection volume for administration [22]. Moreover, the drug must be stable when exposed to varying enzymes and pH *in-vivo* [38].

2.2 Impact of route of administration on *in vivo* behaviour of LA nanoformulations

Drug-loaded nanoformulations when administered parenterally via subcutaneous (SC) or intramuscular (IM) route showed a therapeutic effect for several months. The long-acting effect of these nanoformulations was could be due to the formation of a depot at the site of administration to enable sustain drug release for an extended period. Sequestration of nanoparticles from the depot into lymphocytes [39] or macrophages [8,40] to form secondary depot for long term slow release of the drug is another reason for the long-acting effect. Intravenous infusion has also been utilized for long-acting anti-HIV effects. For instance, Vedolizumab is long-acting humanized immunoglobulin [2-Rmonoclonal antibody which binds to α4β7 integrin and inhibits the virus entering the $CD4^+$ T cells administered as IV infusion for 30 min depicted serum half-life of 25 days [41]. It has been reported that both SC and IM routes showed sustained drug release of nanodrugs independent on particle size [42]. However, the absorption via IM route is fast as compared to SC route, making it suitable for administration of oil based LA nanoformulations. For instance, when pharmacokinetic after IM and SC administration of long acting rilpivirine nanosuspension was compared, it was observed that SC route elicited sustained plasma concentration for 6 months, than IM upto 3 months in beagle dogs. Further, The C_{max} was significantly higher (4.5-folds) with decreased T_{max} (6-folds) for 5 mg/kg IM rilpivirine nanosuspension compared with SC rilpivirine nanosuspension (200 nm). IM administration of rilpivirine nanosuspension led to rapid onset of action due to higher draining effect due to the presence of blood capillaries when compared with SC [43]. While, administration of rilpivirine nanosuspension in humans by SC and IM route led to similar C_{max} while, the T_{max} was 1.83 folds and 7.4 folds higher at 100 mg and 200 mg IM dose, respectively. Therefore, although both the routes led to similar plasma concentration, the duration of action was prolonged by the SC route. The tissue to plasma ratio of rilpivirine administered via SC was 1.25-folds and 1.47-folds higher in the cervix and

vagina, respectively, when compared to IM route [25]. On the contrary, a clinical trial of cabotegravir long-acting nanosuspension in 72 human volunteers demonstrated comparable C_{max} (0.166-0.644 μg/ml) and median half-life of 69 days when administered via both SC and IM route [44]. Therefore, along with the route of administration, other factors including the difference in muscle mass, gender, fat distribution, injection technique, and physical activity might also be the cause of variation in the rate of absorption and maintenance of desired plasma concentration. To conclude, both SC and IM route of administration may provide sustained drug delivery for longer duration and could, therefore, be preferred for LA nanoformulation delivery. However, an enhanced duration of action with increased tissue/plasma ratio could be obtained by administration via the SC route.

2.3 Role of the circulatory and lymphatic system in the enhancement of bioavailability of long-acting anti-infectives

Both circulatory and lymphatic systems play a significant role in the targeted delivery of anti-infective drugs. When high pressure is built in tissues, the blind-ended lymphatic capillaries, which consist of endothelial cells, unidirectional valves open and drain the interstitial fluid into the lymph vessels to thoracic ducts which then accumulated into collecting valves and draining into the left subclavian vein. The hydrostatic pressure head (generally between 0.2-0.8 cmH_2O) is the primary driving force for draining the interstitial fluid into lymphatic vessels [45].

Furthermore, a suction force is also generated during the resting phase of the vessels, which further contributes to the accumulation of interstitial fluid into the lymphatic vessels [45]. In contrast to tight junctions present in the endothelial cells of the blood capillaries, the lymphatic valves are composed of fenestrated endothelial cells, forming a pore of 2 μm. Therefore, large molecules can rapidly enter into the lymphatic system [46]. The lymphatic muscles aid in slow phasic contraction and relaxation of vessels as compared to blood

capillaries (10/min) [47], which could enable longer retention of nanoparticles when absorbed and distributed via the lymphatic system, thereby enhancing the bioavailability of the drug. HIV replication occurs predominately lymphoid organs and lymph nodes throughout the body. It was reported that after treatment with cART in SIV-rhesus macaque for one year, the plasma viral load was suppressed. However, the viral RNA was observed in different organs in the order of lymphatic tissues>lungs and intestine>other tissues [48]. The lymph nodes are a major site of viral hub for replication and retention in germinal cells and CD4+ T cells. Therefore, viral rebound may occur due to viral residues in the lymph node [49]. Increased absorption in the lymphatic system through lymphatic plexus in SC and skeletal muscles, therefore, could enhance the effectiveness of LA nanoformulations. Particle size of nanocarriers has also been reported to play a crucial role in the distribution of LA nanoformulations via the lymphatic system. Upon SC/IM administration, nanoparticles of larger size could form a depot. Depending upon the physicochemical properties, drugs will be absorbed by either the lymphatic or blood circulatory system. For instance, <100 nm particles could be absorbed by the lymphatic system, thereby enhancing circulation time and bioavailability [50]. Macrophage at the injection site engulfed LA nanoformulation passed through the lymphatic system slowly into systemic circulation which resulted in the slow release of drugs from macrophage LA nanoformulation depot [51]. Nanoparticles with a hydrophobic surface and larger particle size (>200 nm) tend to be phagocytosed upon intravenous administration [52]. This strategy can be well explored for long-acting slow release of drugs from macrophages. For instance, higher accumulation of Zidovudine myristate loaded liposomes were observed in reticuloendothelial organs and brain after IV administration due to phagocytosis of liposomes [53]. While, Myocet® which contains Doxorubicin liposomes form macrophage depot upon IV administration causing slow-release mimicking infusion [1]. Dou et al. demonstrated the release of indinavir from the

macrophage-based system for 14 long days and suppressed viral load significantly in the brain after intravenous administration in mice [54]. Nucleoside reverse transcriptase inhibitors (NRTI)and protease inhibitors (PI) have the inherent potential to target endosomes of macrophages and elicit antiretroviral effect [51]. For instance, Atazanavir nanoART led to the highest accumulation in macrophage compared to granulocytes and differentiating cells, further higher concentration of drug was obtained in spleen> liver> lymph node when administered via intraperitoneal and IM route [55]. Therefore, LA nanoprodrug or LA nanocrystal could form effective depot in macrophages which ultimately enter into the lymphatic organs from blood circulation and further enhance half-life and bioavailability of antiretroviral drugs.

3. Long-acting nanoformulations for infectious diseases

The majority of LA nanoformulation has been explored for ARV drugs with few illustrations of anti-malarial and anti-tuberculosis drugs. Various nanoformulations including nanocrystals [6], nano-prodrug [7,8], solid drug nanoparticles [18,56], lipid [10–13] and polymeric nanoparticles [14,15] and nanosuspension [16,17] have been explored for LA ARV effect. The method of preparation and long-acting slow effective release potential of LA nanoformulations have been presented in Figure 1.1. The preceding section deals with LA nanoformulations which have shown promising results in preclinical studies.

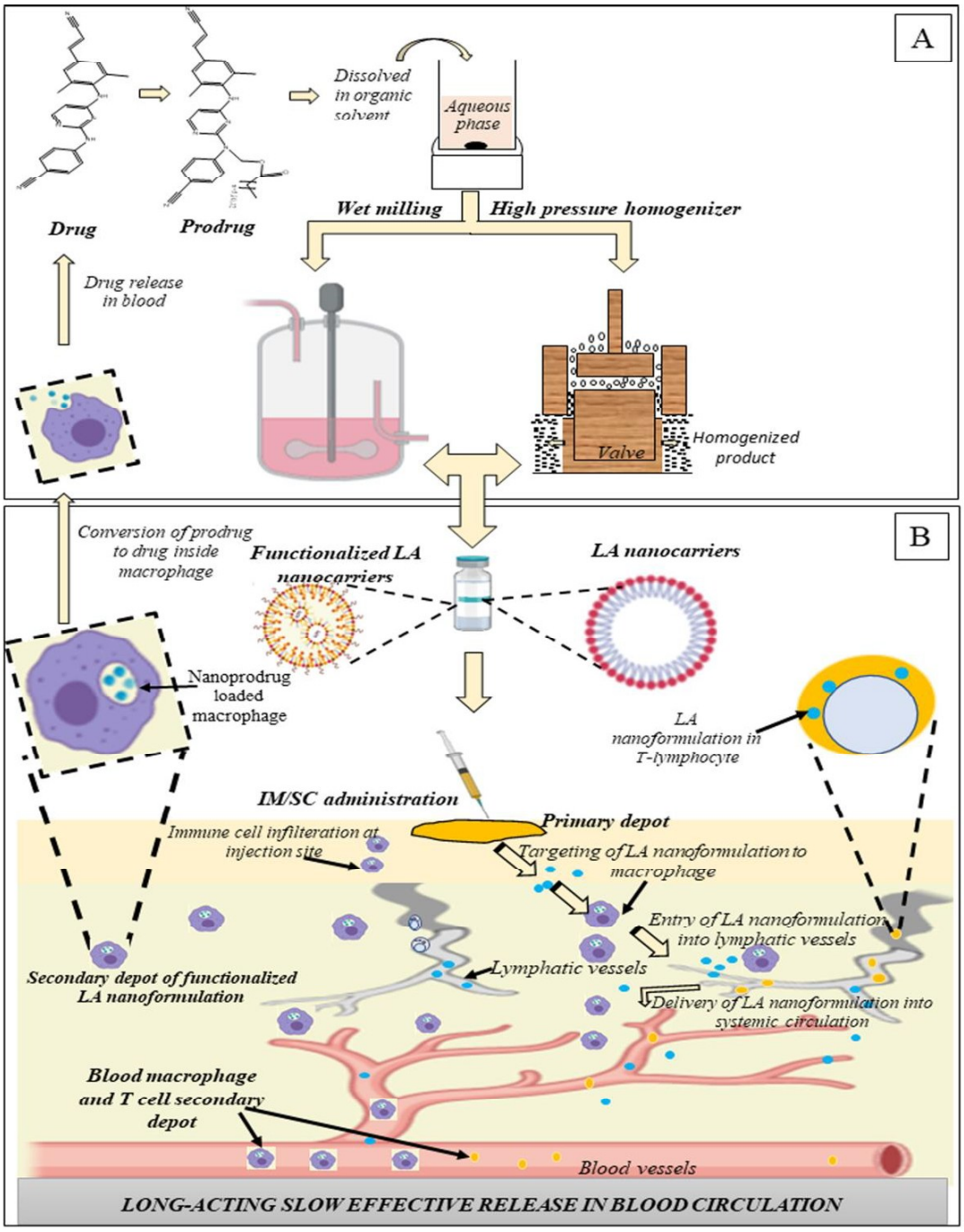

Figure 1.1 Schematic presentation of (A) Method of preparation of long-acting nanoformulations. (B) Mechanism of lymphatic and immune cell targeting of long-acting nanoformulations after subcutaneous or intramuscular administration.

3.1 Long-acting solid drug nanoparticles

SDN are drug/prodrug nanocrystals stabilized with surfactant and exhibit high drug loading (>25% w/w) with extended-drug release profile [57]. Fast regulatory approval (especially, if the drug is FDA approved), long-term stability, improved bioavailability, flexible pharmacokinetic profile, and ability of cellular/tissue targeting are certain advantages of LA SDN [57–59]. Moreover, due to enhanced hydrophobicity and reduced particle size, it revealed a higher intracellular accumulation compared to the free drug [60]. After the successful clinical trials of low dose cabotegravir and rilpivirine nanocrystal nanosuspension, SDN have been explored as a long-acting injectable for sparingly soluble antiretroviral drugs of high doses (150-600 mg BID). For instance, Owen et. al. developed long-acting Maraviroc SDN (750 nm) using polyvinyl alcohol (PVA) and 1,4-bis-(2-ethylhexoxy)-1,4-dioxybutane-2-sulfonate (AOT) with 70%w/w drug loading. *In vivo* IM administration in adult male Wistar rats (10 mg/kg) revealed detectable plasma concentration of Maraviroc SDN up to 240 h in comparison to free Maraviroc solution (5% DMSO) which was detected until only 72 h. The $AUC_{0-\infty}$, terminal half-life and T_{max} was 3.45, 2.64, and 2-fold, higher for Maraviroc SDN compared with free Maraviroc 1-week post-dosing, respectively. Similarly, Atovaquone polymeric solid drug nanoparticles (particle size<1000 nm, PDI<0.4) were developed by the solvent evaporation method. The nanoparticles elicit prevention against malaria up to 7 days when administered via IM route in *P.berghei* ANKA C57BL/6 mice model when compared with free atovaquone administered orally. The prevention was found to be both suppressive and causal in nature [18]. However, SDN needs to be further evaluated to extrapolate the data for other species, to depict its clinical benefits [9,61].

3.2 Long-acting nanocrystals

After the successful advent of cabotegravir and rilpivirine nanocrystal based nanosuspension into phase 3 clinical trial and its subsequent new drug application appeal to FDA by ViiV

Healthcare [62], nanocrystal technology has been enticing for the scientific community for LA nanoformulation development. For instance, preclinical studies of LA nanocrystals (nanoART) of atazanavir (nanoATV) and ritonavir (nanoRTV) depicted LA effect due to tissue macrophage depot when administered in mice and monkeys by SC and IM route, respectively. Acute single dosing of NanoATV revealed 13- and 41-fold higher concentrations in plasma and tissue, respectively, as compared with free ATV. Moreover, multiple dosing (at day 0, 3, and 7) of nanoATV revealed 270-folds higher serum and tissue concentration of ATV compared with free ATV for up to 8 weeks. Both nanoATV and nanoRTV were accumulated in the non-lysosomal compartment of tissue macrophages [6]. To achieve targeted delivery with enhanced macrophage uptake of LA nanoformulation, surface conjugation [63] have been explored. Tissue-specific macrophages, including the liver, spleen, lymph node, gut-associated lymphoid organ, and brain express folic acid receptor (FA-R) onto the cell surface. Targeting of antiretroviral drugs to cell-based and tissue-based FA-R expressing macrophages could enhance LA nanoformulation efficacy. Therefore, nanoART stabilized with folic acid-conjugated poloxamer 407 incorporating atazanavir boosted with ritonavir (FA-nanoATV/r) were developed. The plasma concentration of RTV did not differ between FA-nanoATV/r and nanoATV/r. While the plasma concentration was increased by 2.3-folds for ATV when FA-ATV/r was administered as compared to non-functionalized nanoATV on day 14 post-IM administration. Also, 5-folds increase in bioavailability with a 5-fold reduction in dose of FA-nanoATV/r was obtained [64]. Secondary macrophage depot, along with the injection site depot, was confirmed by a biphasic plasma profile of FA-nanoATV/r. The biodistribution of FA-nanoATV/r in HIV reservoir sites, including spleen, liver, lymph node, kidney, lungs, and plasma were significantly higher compared with nanoATV/r 14 days post-administration. The ratio of CD4/CD8 count was restored by 17% in the case of FA-nanoATV/r (50 mg/kg) treatment

group as against only 3% in PBS treated group in infected mice. FA-nanoATV/r led to a significant reduction in P24 level in the liver and spleen and HIV-1_{gag} RNA levels in the spleen compared with nanoATV/r and untreated group. Therefore, macrophage targeted FA-nanoATV depicted the potential of LA nanoformulations as once biweekly with a 5-fold reduced dose [63]. Similarly, LA anti-malarial nanocrystal suspension have also been attempted recently for Decoquinate. The nanocrystal suspension was prepared by high-pressure homogenization and sonication in peanut oil (particle size: 430 nm). The concentration of Decoqunate remained above its minimum inhibitory concentration up to 624 h in infected mice. The developed nanocrystal suspension depicted causal prophylaxis against P.berghei sporozoite for 2-3 weeks post-IM administration (120 mg/kg) [19]. Similarly, Gallium tetraphenyl porphyrin nanocrystals elicit sustained drug release and reduced the growth of mycobacterium and HIV co-culture in MDM up to 15days [20,65].

3.3 Long-acting nano-prodrug

Monthly/bimonthly LA nanoformulation administration exhibits a major challenge associated with a relatively high dose and volume of administration. Prodrugs could be viable alternatives to further enhance the potency by slow conversion to parent molecule leading to slow effective plasma concentration. For instance, cabotegravir LA nanocrystal nanosuspension requires to divide into two injections (2 ml each) to administer 800 mg dose. Further, in ÉCLAIR trial 2/3rd population had plasma concentration below 4*IC_{90} of cabotegravir, which urges for increased frequency of administration by IM route. Further, the IM cabotegravir depot was rapidly absorbed from the injection site [66]. These observations resulted in the creation of a prodrug of cabotegravir with more hydrophobicity than the parent drug, to prevent fast release, achieving sustained plasma level and decreased dosing regimen. For instance, fourteen carbon myristoylated prodrug of cabotegravir (MCAB) showed 1.24-folds lesser IC_{50} value than cabotegravir against HIV-1_{ADA} in MDM. Nanoformulations of

myristoylated cabotegravir (NMCAB) and cabotegravir (NCAB) were prepared using poloxamer 407 to form rod-shaped particles. These rod-shaped particles could be phagocytosed by macrophage and were stable up to 90 days. Cell uptake studies revealed that NMCAB were phagocytosed by macrophages 60- to 88-folds higher compared with Cabotegravir long-acting parenteral (CAB LAP) formulation and NCAB respectively. NMCAB crystals were observed inside macrophages depicting the conversion of prodrug MCAB to CAB. Treatment with NCAB and CAB LAP showed an increase in RT level by 70 and 84% on day 15 while, NMCAB treatment caused sustained RT inhibition in HIV-1_{ADA} infected MDM cells. IM administration in BALB/cJ mice elucidated sustained plasma level (above 4*IC_{90}) up to day 56 for NMCAB (45 mg/kg) while; it fell below 4*IC_{90} on day 35 in case of CAB LAP. 4-fold higher both plasma half-life and volume of distribution while, a 2-fold increase in mean residence time (MRT) was observed upon NMCAB treatment compared to CAB LAP. Lung, Liver, kidney, gut, and spleen depicted CAB concentration above PA-IC_{90} in NMCAB group, unlike CAB-LAP treated group. Further, in rhesus macaque, the half-life was 2-4 folds higher for NMCAB (45 mg/kg) compared with CAB-LAP (45 mg/kg). Also, secondary tissue depot and immune cell depot of NMCAB were confirmed by higher MCAB concentration in liver, lung, spleen, and lymph node as against blood after 24 h as well as in infiltered immune cells at the injection site. The reduced viral DNA, RNA, and p-24 expressions in tissues were correlated with >5-fold increase in cabotegravir amount in those tissues upon administration with NMCAB. Thus, NMCAB depicted the potential to increase dosing interval with reduced dosage and dosing volume in preclinical findings [7]. Similarly, poloxamer 338 or 407 stabilized N-acylalkoxy rilpivirine (RPV) prodrug nanoformulation (NM3RPV) was synthesized to achieve long-acting slow effective release (LASER) up to 25 weeks. The stability of NM3RPV was comparable with nanoformulated RPV (NRPV) at 4°C and 37°C over 100 days. NM3RPV was retained into

MDM cells for 30 days. While, RPV level, in the case of rilpivirine nanocrystal suspension (NRPV), reduced below the limit of quantification by day 20. Further, >90% viral suppression in HIV-1_{ADA} infected MDM cells up to 30 days when treated with NM3RPV (10 μM and 30 μM) was achieved as against only 67% protection up to day 10 with relapse occurring at day 20 upon NRPV treatment. The plasma concentration of RPV was maintained above PA-IC_{90} value (12 ng/ml) up to 25 weeks as against 16-weeks after IM administration in BALB/cJ mice treated with NM3RPV and NRPV respectively. Further, 13- and 26-folds increase in $t_{1/2,}$ and MRT was observed when treated with NM3RPV. Further, RPV was detected in all the tissues (spleen, lymph node, liver, gut, kidney) after 46 weeks in NM3RPV treated group with the highest concentration in lymph node (145 ng/g) while no RPV was detected in NRPV group. In rhesus macaque, the plasma concentration of NM3RPV was 2- to 16-folds higher compared to RPV up to 44 weeks. Further, detectable levels of RPV and NM3RPV was found in the lymph node, rectal and adipose tissue biopsies at 204 days [8]. Prodrug nanoformulations have also been created to obtain LA slow release for the highly hydrophilic drug by enhancing their hydrophobicity. For instance, palmitoylated emtricitabine (FTC) prodrug nanoformulation (NMFTC) was prepared using poloxamer 407 as a stabilizer by high-pressure homogenization. The prodrug revealed a decrease in aqueous solubility of FTC by 1200-folds and was found to be stable for ten weeks. Further, NMFTC was more effective in suppressing 100% viral load up to ten days when challenged with HIV-1_{ADA} after 8 h. In contrast, only 24 h viral suppression was observed in the case of FTC nanoformulation (NFTC) treated group in HIV-1_{ADA} infected cells. Plasma concentration of FTC was only 5-fold lower than IC_{50} upon IM administration of NMFTC compared to 8-fold lower than IC_{90} with NFTC by day 14 post IM treatment. Biodistribution studies revealed a higher concentration of FTC in the liver, spleen, and lymph node in the NMFTC group up to day 7 with a detectable concentration in the lymph node on day 14 only in NMFTC treated

mice. Further, a significantly higher concentration of FTC-triphosphate (a metabolite of NMFTC) was observed in PBMC and lymphoid cells of the spleen and lymph node. Thus, NMFTC effectively enhanced drug delivery to viral reservoirs with reduced dosing frequency compared to available once-daily oral regimen encompassing the inability to target HIV prone cells [30]. Many other antiretrovirals, including Darunavir [67], Lamivudine [31,68], Abacavir [69], and Dolutegravir [70] have been recently explored for conversion into prodrug nanoformulation with efficient LA slow-release potential in preclinical studies. Pharmacokinetic characteristics of these LA nanoformulations are presented in table 1.1.

3.4 Long-acting polymeric nanocarriers

Polymeric nanocarriers have been widely utilized as long-acting nanoformulations due to the depot formation when administered via SC or IM route. Polymeric LA nanoformulations necessities the use of biodegradable and biocompatible polymers for drug delivery to avoid removal after the exhaustion of drugs. The hydrophobic nature of the polymers is another essential property to enable drug release over an extended period [71]. Further, hydrophobicity of the polymer could enable enhanced absorption of nanoparticles through lipophilic vessels [72]. Moreover, polymeric nanocarriers could encapsulate both hydrophilic [73] and hydrophobic drugs [14,74,75] for long-acting slow-release, by diffusion or dissolution of the drug/s from the polymeric nanocarriers [71]. Recently, efforts were directed to develop polymeric nanocarrier incorporating elvitegravir (EVG), tenofovir alafenamide (TAF), and emtricitabine (FTC) for LA effect to obtain the drug concentration similar to the daily plasma profile of Genvoya*, a marketed product available for HIV treatment. PLGA (lactide: glycolide ratio-75:25) was used to retard the release of hydrophobic (EVG and TAF) and hydrophilic (FTC) drugs for a longer duration. The LA nanoparticles (EVG+TAF+FTC NP) were effective for biweekly SC administration compared to the once-daily pill of Genvoya*, and the plasma viral load was suppressed over 22 weeks. Infra-red dye loaded

PLGA nanoparticle revealed accumulation of nanocarriers in the HIV infection site (female reproductive organ and colon), viral reservoir site (brain and spleen), and infection spread site (subclavicular, axillary and inguinal lymph node) at day 14 post SC administration. Moreover, the potential of nanoparticles for slow effective release was evident by high fluorescence at the injection site and draining organs including liver and kidney even after 14 days. Moreover, EVG+TAF +FTC NP showed 4-fold decrease in plasma viral load up to 22 weeks with maintenance of plasma CD4 level (>80%) until 15 weeks. Viral rebound occurred by 24^{th} week (4 weeks post EVG+TAF+FTC NP SC administration), suggesting need for biweekly administration of (EVG+TAF+FTC) NP. (EVG+TAF+FTC) NP was the the first proof of concept for LA cARV delivery. [15]. Three drug cARV have recently been replaced by two drug combination for pre-exposure (PrEP) prophylaxis. For instance, long-acting polymeric nanoparticles encapsulating TAF+FTC [76] and TAF+EVG [77] were designed to overcome the daily pill burden associated with Truvada® (TAF+FTC) [78]. TAF+FTC PLGA nanoparticles showed higher cell viability (88%) compared to TAF+FTC solution (60%) in TZM b1 cells. The plasma $t_{1/2}$, $AUC_{all,}$ and vaginal tissue $t_{1/2}$ for TAF and FTC were found to increase by 2.2- and 28.33-folds, 4.2- and 19.5-folds and 6.5- and 9.3-folds respectively for TAF+ FTC NP compared with TAF+FTC free solution upon SC administration in CD4 NSG mice. The required vaginal tissue concentration of TAF 14 days post TAF+FTC NP SC administration was 1.6-folds higher than the required TAF vaginal concentration (6.8 ng/g). Interestingly, FTC tended to accumulate in the vagina while both TAF and FTC tended to accumulate in the colon upon SC administration. Further, TAF+ FTC NP (200 mg/kg) depicted 88% (day 4) and 60% (day 7 and 14) protection in Hu CD34 NSG mice when challenged with vaginal HIV-1 strain depicting its long-acting potential with enhanced tissue penetration ability [76]. The synergistic potential of EVG along with TAF was explored by developing long-acting TAF+ EVG PLGA nanoparticles (TAF+EVG NP)

for PrEP [75]. Upon SC administration in $CD34^+$ humanized nice, TAF+EVG NP depicted 8-folds and 5-folds increase in plasma $t_{1/2}$ for TAF and EVG, respectively, compared with their free drug solution. Further, drug concentration in vaginal and colon tissues at day 10 was greater or equivalent to that TAF and EVG concentration, which was obtained at 72 h upon SC administration of TAF+EVG solution. Long-acting PrEP potential of TAF+EVG NP was evident with the increased vaginal AUC by 2.7-3.9 times [77] for both drugs and 100% and 60% protection on day 4 and day 14 post-SC administration in vaginally challenged Hu BLT mice [75].

Long-acting PLGA nanoformulation of rifampicin (RIF) and isoniazide (INH) were developed and evaluated against *M. smegmatis* strain in MDM cells. The nanoparticles depicted 6-fold higher efficacy compared with free RIF and INH. The uptake of RIF and INH co-loaded LA PLGA nanoparticles was 60-folds higher in MDM cells. While the drug release of RIF and INH from LA PLGA nanoparticles occurred till 15 days in comparison to 24 h for free RIF and INH. Furthermore, the RIF and INH nanoparticles reside in the endosomal compartment in MDM cells where mycobacterium persists [21].

3.5 Long-acting lipid nanoparticles

In the case of LA nanoformulations under the late stage of clinical trials, administration of high dose antiretroviral drugs as a single injection is a significant challenge, which requires dividing large injection volume into multiple small volumes to administer the entire dose [79]. Incorporation of poorly soluble drugs in lipid-based nanocarriers (LNP) could be a promising strategy to overcome the above limitation due to enhanced solubilization and drug loading [80–82]. Moreover, lipids are biocompatible and biodegradable [83] and hydrophobic, which could facilitate the intracellular delivery of drugs [84]. LNP can form depot after SC or IM administration, whereby it circumvent blood circulation and enter into the lymphatic system to target HIV residence and spread-sites located in multiple regions

[85] by using reduced dose and small injection volume [46]. Furthermore, cARV with differential physicochemical properties can be encapsulated into lipid nanocarriers. Therefore, a targeted long-acting antiretroviral product 101 (TLC-ART 101 LPV) was designed by incorporating Lopinavir (LPV), Ritonavir (RTV), and hydrophilic Tenofovir (TFV) into DSPC and DSPE-PEG nanocarriers for lymphocyte targeting in non-human primates (NHP) [39]. Improved pharmacokinetic profile with enhanced $AUC_{0-\infty}$ by 2.5, 3.5, and 28-folds for LPV, RTV, and TFV respectively upon TLC-ART101 LPV SC administration was obtained compared with free drug solution in the macaque. Also, the half-life of TLC-ART101 LPV was prolonged by 55.1, 5.1, and 8.2-folds for LPV, RTV, and TFV, respectively. Further, the plasma concentration-time profile of each drug showed short, medium, and long lag time represented as 3-waves, which was predicted due to the entrapment of nanoparticles into lymph nodes, slow drainage from thoracic lymph vessels into blood circulation and drug release from lymphocytes (a secondary depot) [39]. Further, to explore the application of TLC-ART technology, LPV was replaced with second-generation protease inhibitor (atazanavir, ATV). The TLC-ART incorporating ATV, RTV, and TFV combination (ATV-RTV-TFV DcNP) depicted sustained plasma level until 336 h post-SC administration in macaque compared with 48 h when in solution. Enhanced targeting of ATV-RTV-TFV DcNP to PBMC was confirmed with higher AUC_{PBMC} by 33.46-, 1.5, and 5-folds for ATV, RTV, and TFV, respectively, when compared with drug solution [10]. Nevertheless, biodistribution, efficacy, and toxicity profile of LA lipid-based nanoformulations are yet to be established to enable successful translation from lab to clini

Table 1.1 Summary of Pre-clinical pharmacokinetics and efficacy studies of long-acting (LA) nanoformulation for delivery of anti-infective agents

Drug	**Nanocarrier**	**Route**	**Pre-clinical pharmacokinetic parameter and efficacy**	**Animal model for *In vivo* efficacy**	**Ref**
			Solid drug nanocarriers		
Maraviroc	PVA stabilized SDN (750nm;<0.5;70%) First-order kinetics with 22.7% and 10% slower release compared to free Maraviroc in transport buffer and simulated intestinal fluid (SIF)	IM	***Species: Wistar rats*** ***C_{max} (ng/ml)*** / ***AUCt-∞ (ng h/ ml)*** / ***Terminal $t_{1/2}$ (h)*** / ***T_{max} (h)*** Maraviroc SDN: 72.96 / 1959.71 / 140.69 / 2 Free Maraviroc: 71.67 / 567.17 / 53.23 / 1	--	[9]
Atovaquone	PVA or PVP-K-30 SDN stabilized with tween 80 or sodium deoxycholate (<1000 nm, <0.4, +8-20.0 mV)	IM	❖ Plasma concentration was >200ng/ml during challenge after 7 days of administration which correlated well with efficacy. The plasma half-life of atovaquone SDN was determined to be 105 h in mice plasma. Efficacy studies revealed causal protection of SDN upto 28 days when challenged with *P.berghei* at an interval of 7 days in C57BL/6 mice	C57BL/6 mice injected intravenously with *P.berghei* sporozoites	[18]
			Nanocrystals		
Cabotegravir	Polysorbate 20 and polyethylene glycol 3500 stabilized nanocrystal	IM/ SC	***C_{max}(ng/ml)*** IM: 44,900-93,800 SC: 33,700-59,700		[66]

Rilpivirine	Poloxmer 338 or D- α-tocopheryl polyethylene glycol 1000 succinate coated nanocrystal (200nm,400nm,800 nm)	IM/ SC	***Species: rats*** ***C_{max} (ng/ml)*** / ***T_{max} (h)*** / ***$AUC_{t\text{-}last}$ (ng.h/ml)*** / ***BA*** IM (5 mg/kg): 71 / 7 / 3840 / 78 SC (5 mg/ kg): 42 / 3 / 3540 / 72 IM (20 mg/kg): 158 / 7 / 15300 / 78 SC (20 mg/kg): 73 / 7 / 15500 / 78 ***Species: Beagle dog*** IM (5 mg/kg): 619 / 0.5 / 23200 / 102 SC (5 mg/kg): 31.4 / 288 / 19700 / 80 ❖ Pharmacokinetic study in beagle dogs revealed stable plasma concentration (1.4 ng/ml) upto 144 h post-SC administration of Rilpivirine nanocrystal (200 nm) compared with 400 nm and 800 nm. An increase in dose (4-fold) led to a 2-to 2.7-folds increase in plasma exposure. Upon IM administration, peak plasma concentration reached in 24 h with a rapid decline to 5% of C_{max} while SC led to constant plasma level (22 ng/ml) until 24 days. Mean exposure by IM and SC being 41.4 µg h/ml and 24.4 µg h/ml respectively. ❖ Higher Cmax with reduced exposure was observed upon an increase in particle size of nanocrystal from 200 nm t0 400 nm and 800 nm respectively.	--	[33]
Atazanavir (ATV) and ritonavir (RTV)	Poloxamer 188 stabilized nanocrystals Drug release in MDM cells for RTV peaked at day 1 and	SC	❖ ATV concentration reached above MEC (150 ng/ml) within 6 weeks while RTV plasma concentration reached 213 ng/ml in 5 weeks ❖ Liver and spleen concentration was relatively constant (1000-10000 ng/g) upto 8 when nanoART was administered every week for 6	HIV-1_{ADA}intraperitoneally injected in	[86]

	sustained until day 10, in contrast to ATV with peak on day 5 with level below 2 mg/ml on day 10 and 15		weeks ❖ 100-1000 folds reduction in viral load (VL) upto 2500 copies/ml after 4 weekly injections was obtained with viral rebound upon cessation of therapy after 6 weeks with significant neuroprotective effect	$CD34^{+}$HSC NSG humanized mice	
ATV and RTV (nanoART)	Poloxamer 188 stabilized nanocrystals	SC	After Chronic dose (day 0, and 7) dose (10 mg/kg) SC administration on day 14 the tissue concentration was: ***Species: mice*** ***AUC_{last} (ng.h/ml)*** / ***$t_{1/2}$ (h)*** / ***V_{β} (L/kg)*** / ***Cl (L/h/Kg)*** / ***$MRT_{0-\infty}$*** *Free ATV*: 6,164.4 / 253.3 / 1,933.0 / 5.29 / 120.9 *nanoART-ATV*: 12,592.5 / 1,152.5 / 1,106.8 / 0.67 / 171.6 *Free RTV*: 8,028.0 / 83.6 / 731.4 / 6.06 / 63.5 *NanART-RTV*: 13,586.4 / 230.1 / 771.4 / 2.32 / 142.5 ❖ When nanoART containing ATV and RTV were injected in monkeys, plasma concentration above 100 ng/ml was detected upto 14 days. While in Balb/cJ mice the concentration was 13,41 and 4500-folds higher compared to native drug in plasma, tissue and injection site respectively after single IM dosing. ❖ Multiple chronic dosing showed 270-folds higher serum and tissue concentration upto 8 weeks	--	[6]
ATV boosted RTV (ATV/r)	Folic acid functionalized poloxamer 407 stabilized nanocrystals (FA-P407-ATV/r) (FA nanoATV-374±3 nm;0.23±0.01; -14.0±0.6 mV) (FAnanoRTV-390.1±22nm; 0.21±0.01; -6±10 mV)	IM	❖ Plasma concentration in Balb/cJ mice was above MEC for ATV 14 days post-administration. Tissue ATV concentration was 37.11- and 3.79-folds higher while RTV concentration was 3.57- and 1.28-folds higher with FA-P407-ATV/r compared to P407-ATV/r. The bioavailability was 5-folds higher for FA-P407-ATV/r compared to P407-ATV/r ❖ Infected mice depicted restoration of CD4/CD8 ratio in blood and	Hu-PBL intraperitoneally injected in NOD/SCID/ $IL2R\gamma c^{-/-}$ mice	[63]

			spleen after treatment which was significantly higher compared to control. Also, The HIV p24 content was significantly lower (<2%) when treated with FA-P407-ATV/r compared to P407-ATV/r group.		
Decoquinate (DQ)	DQ dispersed in Peanut oil (430 nm)	IM	❖ IM administration in mice at 120 mg/kg dose led to $t_{1/2}$, C_{max}, AUC, Vd and Cl of 751.01 h, 36.58 ng/ml, 10,385 ng.h/ ml, 12156 L/kg, 11.56 L/h/kg.c Minimum prophylactic dose of LA DQ nanocrystal was found to be 120 mg/kg with protection upto 2 weeks. While 240 mg/kg dose could provide a prophylactic effect upto 8 weeks when tested in C3H murine model challenged with *P.berghei* sporozoites.	C3H murine model challenged intravenously with *P.berghei* sporozoites	[19]
Gallium (GA)	P407 stabilized GA nanoparticles (305 nm; 0.29; +35 mV)	--	--	--	[20]
			Nanoprodrug		
Myristoylated cabotegravir (MCAB)	Poloxamer 407 stabilized nanocrystals (NMCAB-318±25 nm;0.21±0.02; -22±3.4 mV) (NCAB-315±26 nm;0.28±0.04; -8.2±1.4 mV) (CAB LAP-257±6 nm;0.22±0.02;-23.2±1.7 mV)	IM	***Species: Mice*** ***$t_{1/2}$ (h)*** ***$AUC_{0-\infty}$ (h ng/mL)*** ***$V_{\beta/F}$ (L/Kg)*** CAB LAP 71.3±1.2 6884479.4 ±511007.1 0.69±0.06 NM CAB 277.8±5.9 6897132.5 ±260736.5 2.64±0.13 ❖ When administered in male Balb/cJ mice intramuscularly NMCAB was above 4*PA-IC_{90} for 28 days, In male macaques administration of NMCAB led to 2-4 folds higher $t_{1/2}$ compared to CAB LAP. The tissue concentration in brain, liver, spleen, lung, lymph node and kidney was above IC_{90}(166 ng/g) in all organs administered with NMCAB compared to CAB LAP ❖ 9-folds and 6.2-folds higher viral suppression was obtained after administration of NMCAB and CAB LAP respectively. 3log_{10} higher viral DNA, RNA was obtained after treatment with NMCAB	Hu-PBL reconstituted NSG mice	[7]

			in all tissues after treatment with which correlated with >5 fold increase in Cab concentration.		
Palmitoyl fatty acid conjugated emtricitabine (NMFTC)	Poloxamer 407 stabilized nanoprodrug (350±10 nm;0.24±0.02;-20±0.2 mV;90%)	IM	❖ MDM cell challenged with HIV-1_{ADA} showed 100%and 25% protection after 10 and 15 days post-NMFTC treatment. Whereas only 30% protection upto 24 h was obtained after treatment with FTC. ❖ 2-fold and 8-folds higher plasma FTC-triphosphate level was observed in rats after 1 and 7 days post-treatment with NMFTC compared with FTC. 2-4 fold higher splenocyte and lymph node concentration of FTC-TP was also observed on day 1& 7 as against FTC group.	--	[30]
Myristoylated Dolutegravir (MDTG)	surfactant stabilized nanoprodrug (309.7±31.7 nm;0.22±0.03;-20.3±1.8 mV)		***Species: rhesus macaque*** ***Λ (h^{-1})*** | ***$t_{1/2}$ (h)*** | ***$AUC_{0-\infty}$ (h ng/mL)*** | ***$V_{\beta/F}$ (L/Kg)*** | CL /F(ml/Kg) | $MRT_{0-\infty}$ DTG: 0.0015±0.0001 | 467.1±28.1 | 249,640.2±35.707.7 | ND | ND | 691.7±98.4 MDTG: 0.0016±0.0002 | 458.2±55.7 | 41,937.7±16.271.1 | 835.5±334.0 | 1.19±0.36 | 454.6±62.5 ❖ Plasma concentration was above PA-IC90 of 64 ng/ml for 35 days and above 10 ng/ml for 91 days after a single IM dose(118 mg/ml)	--	[87]
Stearoylated Darunavir (NMDRV)	Poloxamer 407 stabilized nanoprodrug (NDRV-384.5±10 nm;0.27±0.01;-7.78±0.36 mV) (NM2DRV-149±2nm;0.26±0.01;-1.74±0.01 mV)	IM	❖ Amine modified Darunavir prodrug led to no HIV RT activity until 30 days when treated with NMDRV and upon HIV-1_{ADA} challenge in MDM cells as against free DRV showing HIV RT activity from day 5.	--	[67]

			Species: male Balb/cJ mice ***Concentration (day 28)*** NDRV NM2DRV Plasma ND 8.4 ng/ml Spleen <3 ng/g 8216.5±1745.2 ng/g Liver ND 1516.8±217.2 ng/g Lymph node <3 ng/g 26848.7±15689.5 ng/g Brain ND 12.2±3.5		
Phosphoramidate Lamivudine ProTide (NM23TC)	Folic acid conjugated nanoprodrug (FA-NM3TC) (189.5±6.1 nm;0.26±0.01;-21±0.2mV; 72%) In MDM cells M23TC released Lamivudine triphosphate at 1685 ng/ml at day 1 and 229.6 ng/ml at day 30 while, no detectable drug was found in native drug treated cells	IM	❖ MDM cells when challenged with HIV-1_{ADA} upto day 30 after treatment with NM23TC for 8h, showed 6.1% and 16% breakthrough on day 20 and 30 in contrast to 24h upon treatment with free 3TC. ❖ FA-NM3TC depicted 1.1-folds higher anti-HIV RT activity in MDM cells. ❖ Sustained plasma drug concentration upon IM administration of NM23TC upto 1 month in contrast to 3TC which fell below the limit of quantitation in day 7. Spleen and lymph nodes served as drug depots. ❖ Plasma, liver, spleen, and lymph node drug level was 2-folds higher at day 5 and 14 after administration of FA-NM3TC compared to NM3TC.	--	[31,68]
Myristoylated Rilpivirine (NM3RPV)	Poloxamer 338 stabilized nanoprodrug (NRPV-277±9nm;0.24±0.02;-9.2±0.3 mV) (NM3RPV-345±5 nm;0.18±0.06;-17.6±0.6 mV)	IM	❖ MDM cells challenged with HIV-1_{ADA} post 8 h after treatment with NM3RPV or NRPV led to >96% protection until 30 days and 67% protection after 10 days t both 10 and 30 µM. ❖ Single IM injection of 45, 75, and 100 mg/kg in male Balb/cJ mice caused sustained plasma level (above PA0IC_{90} 12 ng/ml) until 25 and 7 weeks for NM3RPV and NRPV respectively. 13 and a 26-fold increase in plasma half-life and mean residence time (MRT) was observed for Nm3RPV compared to NRPV. Spleen, liver, and lymph node were substantial depot of M3RPV upto 46 weeks. ❖ In rhesus macaque, IM administration led to 2 to 16-folds higher	--	[8]

			NM3RPV level compared to NRPV with rectal, lymph node and adipose tissue containing detectable drug upto 204 days		
Carbonate and carbamate masking semi-solid emtricitabine prodrug (SSPN)	Polymer coated nnoprodrug (<250 nm;<0.2)	--	❖ PBPK modeling predicted steady plasma concentration for 28 days after reaching C_{max} withing 24h	--	[88]
Abacavir pronucleotide (NM3ABC)	Poloxamer stabilized nanoprodrug (329±3 nm; 0.28±0.01;-45.0±0.4 mV;47.4%) Sustained drug release from MDM cells upto 30 days (100 Fmol/10^6 cells)		❖ Administration of NM3ABC (100μM) led to sustained viral suppression for 15 days, 90% inhibition till day 20 which was reduced to 83% on day 30 when MDM cells were challenged with HIV-2_{ADA}	--	[69]
			Polymer and lipid nanoparticles		
Emtricitabine (FTC)	PLGA nanoparticle (FTC-NP) (175.9±24.7 nm; 0.145±0.028; -25.6±1.94 mV; 53.8±5.07%) Drug release at pH 5.5 suggested 62% FTC release in 1 h, therafter constant drug release was obsereved with only upto 85% FTC release on day 30	- -	❖ HIV-1 positive TZM-b1 cells treated with FTC-NP depicted 43-folds higher efficacy compared to free FTC. Further, FTC-NP depict similar exogenous HIV-1 inhibition in PBMC compared to free FTC solution.	--	[73]
Bictegravir (BIC)	PLGA nanoparticles (BIC NP) (189.2±3.2 nm;<0.2;-24.3±3.9 mV; 47.9±6.9%) 45% BIC release at pH 5.5 in	--	❖ *In vitro* pharmacokinetic revealed 2.4- and 3.1- times higher BIC-NP compared to BIC solution in TZM-b1 cells ❖ BIC NP depict 159 times and 30 times higher efficacy in TZM-b1 and PBCM cells infected with HIVNLX and HIV ADA	--	[74]

	1 h after which constant release was observed upto 72% on day 14		respectively compared to BIC solution ❖ The selectivity index in TZM-b1 and PBMC was 215,789 and 523.33 for BIC-NP compared to 3.7 and 1.5 respectively.		
Compound 1 (Comp)	PLGA nanoparticle (Comp NP) (370±9.2 nm;<0.2;-28±0.1 mV;95±9.1-104±26.2%)	IP	***Species: Balb c/J mice*** ***AUC0-last (µg.h/mL)*** / ***CL, ml/min/kg*** Comp (20 mg/kg): 209.2±23.8 / 1.5 Comp NP (20 mg/kg): 472.9±20.99 / 0.7 ❖ Complete inhibition of HIV-1 infected TZM-b1 cells was observed upto day 35 when treated with Comp NP as against 4 h for Comp 1 ❖ Intraperitoneal administration of Comp NP led to a 100-fold greater plasma concentration compared to EC_{50} for WT HIV-1. ❖ Upon injection of compound 1 (100 mg/kg) and comp NP (190 mg/kg) intraperitoneally in HIV-1 infected humanized NOD.*Cg*-Prkdc^{SCID}Il2rg^{tm1wjl}/*Szj* mice depicted 10^4 plasma viral load on day 8 in compound 1 group and no VL upto 19 days in Comp NP group with an increase to 10^4 and 10^5 on day 25 and 32.	HIV-1 infected humanized NOD.*Cg*-Prkdc^{SCID}Il2rg^{tm1wjl}/*Szj* mice	[14,89]
Elvitegravir (EVG)+ tenofovir alfenamide (TAF)+emtricitabine (FTC)	PLGA nanoparticles (PLGA cARV NP) (243.2±5.8 nm;<0.2;-20.73±9.3 mV;38.6±2.9%(EVG),50.7±2.6 (TAF), 46.4±3.6 (FTC))	SC	❖ Plasma viral load was undetectable after the third biweekly dose of cARV NP administered SC with a detectable concentration of each drug in the lymph node and female reproductive tract at week 22.	Humanized BLT mice	[15]
ATV, RTV and Tenfovir (TFV)	DSPC and DSPE-mPEG2000 (DcNP) (6-62 nm;99±8.2% (ATV),92±7.1% (RTV),10±0.8% (TFV))	SC	❖ Sustained drug concentration upto 336 h was obtained for ATV, RTV, and TFV in plasma and upto 336 h and 192 h for ATV,RTV, and TFV respectively in PBMC upon DcNP administration compared to free drug wherein drug concentration lasted for 48h		[10]

			after SC administration in macaque. ❖ The AUC was 5 and 35 folds higher and Clearance was 4- and 23-folds lower for ATV and TFV respectively, $t_{1/2}$ was 110-,17- and 7-fold higher for ATV, RTV, and TFV respectively when DCNP was administered SC compare to free drug. The lymph node mononuclear cells showed a 3-fold higher concentration of ATV and RTV when administered through DcNP compared to free drug. ❖ MBPK modeling depicts slower lymphatic passage for ATV and RTV compared to TFV. Also, it predicted a 2-week dosing interval in macaque depicting long-acting potential.	
TAF+EVF	PLGA nanoparticles (TAF+EVG NP) (190.2±1.7 nm;0.14±0.01;-19.2±1.7 mV;54.1±3.6% (TAF), 44.6±2.4% (EVG))	SC	***Species:Hu-CD34-NSG mice*** ***$AUC_{0\text{-}lastconcn}$ (μg.h/mL)*** / ***$t_{1/2}$*** TAF 14.1±2.0 / 14.2 h TAF-NP 23.11±4.4 / 5.1 days EVG 7.2±0.8 / 10.8 h EVG-NP 39.7±6.7 / 3.3 days ❖ Vaginal AUC was 2.7-3.9 folds higher for TFV and EVG compared to the vaginal AUC when in solution. ❖ TAF+EVG NP depicted 390-folds increased potency compared to TAF and EVG solution ❖ When mice treated with TAF+EVG NP were challenged with HIV-1, 100% viral protection was observed at day 4 and at day 14, 60% protection was elicited	NOD/SCID/ IL2rgnull, CD34-NSG mice	[75,77]

TAF and FTC	PLGA nanoparticles (TAF+FTC NP) (233.2±12.8 nm; 0.11±0.05; -19.1±4.1 mV;69.2±14.5 (TAF),65.9±18.2 (FTC)) Drug release in endosomal pH revealed 73% total TAF and FTC release within 30 min with effective time constant of 22.6 and 15 min respectively.	SC	***Species: Hu-CD34-NSG mice***	Hu-CD34-NSG mice	[76]

Plasma

	C_{max} *(ng/mL)*	AUC_{all} *(Day.µg/mL)*	*CL (L/day/kg)*	V_d *(L/Kg)*	*t/2 (h)*	MRT_{last} *(h)*
TAF	942±137	0.6± 0.08	33.50	285.3	14.2	13.4
TAF-NP	15,954±2716*	2.5± 0.4	78.7	145.6	30.8	13.5
FTC	850±242	0.2± 0.05	1031	149.3	2.4	5.9
FTC-NP	34,026±3140*	3.9± 0.8	49.7	204.3	68.4	13.5

Vagina

TAF	4.0±1.1	2.2± 0.4	92,448	39,558	6.5	10.0
TAF-NP	58.4± 23.4*	10.9±2.1	18,345	46,675	42.3	26.3
FTC	4.5±1.0	1.6± 0.4	118,762	91,640	12.8	11.2
FTCNP	54.1±13.2*	5.4±1.1	35,791	256,605	119.3	13.6

*-p<0.05 compared with free drug solution

- ❖ 80% protection was obtained upon challenging hu-CD34-NSG mice with HIV-1 on day 4 after treatment with TAF+FTC NP at day 0, while it reduced to 60% on day 7 and 14.

ATV, RTV and Efavirenz (EFV)	$mPEG_{2000}$ DSPE (ATV+RTV+EFV nanoART) (281-470 nm;0.200-0.288;-31.6--13.5 mV)	SC	❖ Upon treatment with nanoART after 12 h of infection with HIV-1_{ADA} in NSG mice, ATV and RTV level was above MEC for ATV and RTV in humans (150 ng/ml) on day 14, but the EFV concentration was 4-6 folds lower compared to its MEC. ❖ HIV-1 p24 was significantly decreased while the viral gene level was decreased by 3-order of magnitude in blood when treated with ATV+RTV+TFV nanoART compared to ATV+RTV treatment.	HIV-1_{ADA}infected PBL-NSG mice	[64]

TFV, RTV and Lopinavir (LPV)	DSPC and DSPE-mPEG2000 (TLC-ART 101 LPV)	SC	***Species: Rhesus macaque***	-- [39]

	$AUC_{0-24\ h}$ ***(h*µg/mL) (mean± %CV)***	$t_{1/2}$ ***(h) (mean± %CV)***	***CL/F (L/h/Kg) (mean± %CV)***	$MBRT_{0-24\ h}$ ***(h) (mean± %CV)***
LPV	4.35±7	8.65±28	4.64±14	10.83±5
RTV	1.37±9	7.99±38	4.23±15	10.78±5
TFV	14.4±4	8.01±51	0.72±4	2.61±12
TLC-ART 101 LPV				
LPV	10.98±48	476.94± 173	0.85±85	116.09±8
RTV	4.80±57	44.06±46	1.43±56	24.86±9
TFV	416.55±15	65.33±11	0.02±15	102.68±7

ATV, RTV and TFV	DSPC and DSPE $mPEG_{2000}$ lipid drug nanoparticle (LDN) (63.6±1.1 nm;85.5±8.2% (ATV),85.1±7.1% (RTV), 6.1±0.8% (TFV)) ATV showed pH dependent release with almost 100% drug release within 24 h at pH 3.	SC	❖ SC administration of ATV (25 mg/kg), RTV (12.8 mg/kg) and TFV (15.3 mg/kg) led to sustained plasma concentration upto 7 days in primates.Only 20% of total AUV was attributed to early phase (0-8h) for all 3 drugs.	-- [11]
LPV, RTV and TFV	DSPC and DSPE $mPEG_{2000}$ lipid nanoparticle (LNN) (52.4±9.1 nm;93.6±5.5% (LPV),90.7±7.4% (RTV),11.9±3.0% (TFV))	SC	***Species: macaque***	-- [12,13]

	AUC_{0-168h} ***(µg.h/mL)***	
	Free drug	***LNN***
LPV	3.83±4.04	69.6±10.7
RTV	1.39±1.18	19.4±12.2
TFV	56.6±17.04	395.0±344.5

Values in round bracket indicate particle size; polydispersity index; zeta potential; % entrapment efficiency; nm-nanometer and mV-millivolt; BA-bioavailability

4. Long-acting nanoformulations: challenges and future perspective

The LA effect of nanoformulation grounds on their established physicochemical properties. Retention of these physicochemical properties during the translation from lab to clinic with continuous manufacturing process remains elusive [90]. LA nanoformulation demands the ability to incorporate drugs with different physicochemical properties using single platform technology for its clinical application. However, differential drug release of the ARV [39], drug-drug interaction, and felicity of common carrier remains major defiance [91]. Techniques to establish sterility of LA nanoformulation to maintain equipoise with its stability during manufacturing and storage are yet to be established [92]. Moreover, although the secondary immune cell depot causes a long-acting effect, toxic metabolites when LA nanocarriers are directed towards cellular endosome with acidic pH needs to be thoroughly investigated along with tissue and plasma pharmacokinetic and biodistribution. Nanosuspension, specifically, nanocrystals tend to cause Ostwald ripening and depict polymorphism [42], affecting their solubility and *in vivo* performance, which until now have not been studied for LA nanoformulations. Additionally, the majority of ARV are administered in higher doses, making them unsuitable for LA nanoformulations due to issues regarding dose-volume [93], syringeability, stability, and depot consistency. A standard platform technology may aid in the presentation of anti-infectives to individuals with distinct physiology establishing horizon for personalized regimen inhibiting drug resistance [24,94]. A combination of substantial modification in the viral genome along with a long-acting cART regimen may serve as an excellent remedy in complete eradication of chronic HIV infection soon [95]. Also, the effect on pathogen levels upon non-adherence of LA nanoformulations remains to be established in the near future.

5. Rationale of the present work

Recently, LA injectable nanoformulations have achieved cornerstone due to their ability to slack dose administration with protracted drug delivery at the desired site [1]. Although, this nanotechnology holds value specifically for treatment and prophylaxis of infectious diseases including HIV [96], tuberculosis [21], trypanosomiasis [97], and malaria [18] which requires long-term drug administration to eliminate the pathogen and prevent relapse; yet the technology is prefatory in this area. Therefore, current research work involved the development and evaluation of LA nanoformulations for targeted delivery of antiretroviral and anti-trypanosomal drugs. Recently, few LA nanoformulations for infectious diseases have been established; however, none could present the significance of physicochemical properties of drugs in appropriate selection of nanocarriers and their effect *in-vivo*. To this end, current research revealed the purpose of developing polymer-lipid hybrid nanoparticle and solid lipid nanoparticle for challenging antiretroviral (Efavirenz and Enfuvirtide) and anti-trypanosomal (Isometamidium chloride) drugs, respectively; with varied physicochemical properties as well as half-lives.

Many existing anti-infective agents encompass shorter half-life ($t_{1/2}$) and require daily administration; however, such drugs possess a major challenge of incorporation into nanocarriers eliciting protracted drug delivery for weeks/months [96]. Until now, only Tenofovir ($t_{1/2}$-17 h) and Emtricitabine ($t_{1/2}$-10 h) have been incorporated into LA nanoformulations [76,98]. However, the development of LA nanoformulations for drugs with short $t_{1/2}$ (<10 h) remains unattempted. We, therefore, developed LA nanoformulation of novel combination incorporating drug with a short half-life and higher water solubility (Enfuvirtide; Enf) in combination with hydrophobic and longer half-life antiretroviral (Efavirenz; Efa). Enf is a fusion inhibitor peptide approved by USFDA in 2003 [99]. It is a 36- amino acid peptide with a molecular weight of 4.5 KDa which blocks the fusion of viral

and cell membranes by binding to glycoprotein-41 with poor oral bioavailability [100] and rapid catabolism by peptidase and proteinase prominently in hepatic and kidney cells [101,102]. It has short $t_{1/2}$ of 3.8 h. Previously, *in situ* forming implant [103] and lipopeptide based prodrug approach [104] were ventured; however; there are no reports for combination delivery of Enf with other anti-retroviral drugs encompassing differential physicochemical properties and eliciting LA potential.

Moreover, the development of LA nanocarriers for charged hydrophilic moieties with meagre plasma retention ability and quick disposition and/or elimination is still arduous. However, the majority of anti-trypanosomal agents in the market are charged molecules with very low plasma half-life and rapid disposition. ISMM (M.W. 496 g/mol) [105] is a representative anti-trypanosomal drug which is amphiphilic cationic moiety [106] with rapid disposition in the liver and kidney and inefficient plasma concentration[107]. It was found to have half-lives of 0.13, 1.22, and 120.7 h as determined by tri-exponential equation upon intravenous administration in cattle [108]. Although previous attempts were made in the development of polymeric nanoparticles for ISMM with low hemolytic potential [109]. Development of LA nanoformulation for ISMM with enhanced plasma half-life as well as infection-, spread-, and reservoir-site depot remained elusive. Therefore, current research work aimed to develop solid lipid nanoparticles with the ability to enhance ISMM loading and LA potential. Additionally, current research work involved the establishment of the significance of route of administration for the genesis of primary (injection site) and secondary (infiltered immune cells and tissue macrophage) depot which are desirable to cause protracted drug release.

6. The objective of the present work

Peripheral blood mononuclear cells (especially macrophage) are established primary defence cells that encounter the pathogens upon exposure. Furthermore, they are entrenched hub for residence and replication of pathogens. Therefore, current research work was focused on the

development of nanocarriers which form depot in these primary cells and elicit long-term protection against infectious diseases specifically; HIV and trypanosomiasis. Route of administration circumscribe a significant role in the formation of immune cell depot. SC or IM administration cause infiltration of peripheral blood mononuclear cells emanating secondary immune cell depot which traverses through lymphatic vesicle, sequester into the lymph node, and later drain into systemic circulation preceding thoracic duct. Whereupon, reaching various organs through systemic circulation, they form secondary tissue depot [39]. This leads to improved pharmacokinetics and tissue kinetics leading to protracted drug release. Therefore, current research predominantly involved two aims:

I. Development and evaluation of LA polymer-lipid hybrid nanoparticles (PLN) incorporating novel combination with varied physicochemical properties namely; Efa (first-line non-nucleoside reverse transcriptase inhibitor; NNRTI) and Enf (fusion inhibitor peptide).

II. Development and evaluation of LA lipid nanoparticles (LNP) for hydrophilic cationic Isometamidium chloride (ISMM) with the ability to elicit protracted plasma drug release.

The above aims were achieved by the following specific objectives:

Objective i: Development and validation of analytical/bioanalytical method for quantification of Efavirenz, Enfuvirtide and Isometamidium chloride

The current objective involved the development of a suitable analytical method for estimation of each drug from nanoformulations and release media to determine % drug loading (% DL), % entrapment efficiency (% EE), and % drug release. Therefore, RP-HPLC and spectrophotofluorimetric method was developed and validated for quantification of Efa and Enf, respectively. Further, another RP-HPLC method was developed and validated for the estimation of ISMM in presence of formulation excipients and release media. It further involved the development and validation of a suitable bioanalytical method for estimation of

ISMM from plasma and various tissues to establish the pharmacokinetics and biodistribution profile of developed LA nanoformulation. RP-HPLC method involving a novel ion-pairing approach was developed and validated for the estimation of ISMM from biological matrices after extraction by protein precipitation method.

Objective ii: Optimization, *in vitro* characterization, cellular uptake and biodistribution of Efavirenz and Enfuvirtide co-loaded polymer-lipid hybrid nanoparticles

The current objective involved the creation of LA Efa and Enf co-loaded polymer-lipid hybrid nanoparticles (Efa-Enf PLN) with an ability for simultaneous delivery of both drugs despite their differential solubility as well as enhanced secondary depot genesis ability in immune cells. Efa-Enf PLN were prepared by double emulsion solvent evaporation method and characterized for % EE, particle size (PS), polydispersity index (PDI) and *in vitro* drug release. These parameters have significance in determining the cytotoxicity and cellular interaction of developed Efa-Enf PLN. Furthermore, DSC, FTIR, CD analysis of peptide, and blood compatibility studies were done to conclude on drug-excipient compatibility, stability of peptide in PLN, and *in vivo* safety of developed Efa-Enf PLN. Furthermore, cytotoxicity and cellular uptake studies in macrophage and T-cells were carried out to predict the interaction of Efa-Enf PLN with primary immune cells. Additionally, *in vivo* biodistribution profile for developed LA Efa-Enf PLN was established by bioimaging in Balb/c mice. The biodistribution profile was extrapolated to predict the desirable dose for accomplishing minimum effective concentration (MEC) of Efa and Enf in each organ by mathematical modelling.

Objective iii: Development, *in vitro* and *in vivo* evaluation of long-acting solid lipid nanoparticles for cationic hydrophilic drug (Isometamidium chloride)

ISMM was selected as a representative illustration of a charged hydrophilic drug. The objective involved the development of LA ISMM loaded solid lipid nanoparticles (ISMM-DS

LNP) with improved plasma retention ability as well as enhanced target tissue concentration. Higher drug loading being a prerequisite for LA nanoformulations; therefore, ISMM LNP were prepared by novel *in situ* complexation solvent evaporation method to enhance the drug loading. The ISMM complex was formed using an anionic complexing agent (docusate sodium, DS) and characterized by FTIR to estimate the extent of complex formation. The ISMM-docusate sodium complex loaded LNP (ISMM-DS LNP) were characterized for % EE, particle size (PS), polydispersity index (PDI), zeta potential, *in vitro* drug release, haemolysis, and cytotoxicity in Vero cells. Furthermore, the LA protracted plasma drug delivery of ISMM-DS LNP was evaluated by SC administration in Wistar rats. Moreover, the concentration of ISMM in PBMC at day 7 after SC administration of ISMM-DS LNP and during cell uptake studies in THP-1 cells was determined. Furthermore, the biodistribution profile of ISMM-DS LNP was established by determining the ISMM concentration in different tissues including the liver, spleen, kidneys, lymph nodes, lungs, and brain after 7 days in Wistar rats.

References

[1] Injectable Nanomedicines – New Developments in Long-Acting Injectable Nanoformulations, Drug Dev. Deliv. (2018). https://drug-dev.com/injectable-nanomedicines-new-developments-in-long-acting-injectable-nanoformulations/ (accessed August 4, 2020).

[2] Introduction to Long-Acting Injectables, (2016). https://www.thebodypro.com/article/new-hiv-prevention-model-published (accessed August 5, 2020).

[3] A. Mcivor, H. Koornhof, B.D. Kana, Relapse, re-infection and mixed infections in tuberculosis disease, Pathog. Dis. 75 (2017) 1–16. doi:10.1093/femspd/ftx020.

[4] K. Prayag, D.H. Surve, A.T. Paul, S. Kumar, A.B. Jindal, Nanotechnological interventions for treatment of trypanosomiasis in humans and animals, Drug Deliv. Transl. Res. 10 (2020) 945–961.

[5] Janssen Announces Health Canada Approval of CABENUVA™, the First Long-Acting Regimen for the Treatment of HIV, (2020). https://www.jnj.com/janssen-announces-health-canada-approval-of-cabenuva-the-first-long-acting-regimen-for-the-treatment-of-hiv (accessed May 11, 2020).

[6] N. Gautam, U. Roy, S. Balkundi, P. Puligujja, D. Guo, N. Smith, X. Liu, Preclinical Pharmacokinetics and Tissue Distribution of Long-Acting Nanoformulated Antiretroviral Therapy, Antimicrob. Agents Chemother. 57 (2013) 3110–3120. doi:10.1128/AAC.00267-13.

[7] T. Zhou, H. Su, P. Dash, Z. Lin, B. Laxmi, D. Shetty, T. Kocher, A. Szlachetka, B. Lamberty, H.S. Fox, L. Poluektova, S. Gorantla, J. Mcmillan, N. Gautam, R.L. Mosley, Y. Alnouti, B. Edagwa, H.E. Gendelman, Creation of a nanoformulated cabotegravir prodrug with improved antiretroviral profiles, Biomaterials. 151 (2018) 53–65. doi:10.1016/j.biomaterials.2017.10.023.

[8] J.R. Hilaire, A.N. Bade, B. Sillman, N. Gautam, J. Herskovitz, B. Laxmi, D. Shetty, M.S. Wojtkiewicz, A. Szlachetka, B.G. Lamberty, S. Sravanam, H.S. Fox, Y. Alnouti, P.K. Dash, J.M. Mcmillan, B.J. Edagwa, H.E. Gendelman, Creation of a long-acting rilpivirine prodrug nanoformulation, J. Control. Release. 311–312 (2019) 201–211. doi:10.1016/j.jconrel.2019.09.001.

[9] L.M. Tatham, A.C. Savage, A. Dwyer, M. Siccardi, T. Scott, M. Vourvahis, A. Clark, S.P. Rannard, A. Owen, Towards a Maraviroc long-acting injectable nanoformulation, Eur. J. Pharm. Biopharm. (2018). doi:10.1016/j.ejpb.2018.04.009.

[10] S. Perazzolo, L.M. Shireman, L.A. Mcconnachie, J.C. Kraft, D.D. Shen, R.J.Y. Ho, Three HIV Drugs , Atazanavir , Ritonavir , and Tenofovir , Coformulated in Drug-Combination Nanoparticles Exhibit Long-Acting and Lymphocyte-Targeting Properties in Nonhuman Primates, J. Pharmceutical Sci. 101 (2018) 1–10. doi:10.1016/j.xphs.2018.07.032.

[11] J. Duan, J.P. Freeling, J. Koehn, C. Shu, R.J.Y. Ho, Evaluation of Atazanavir and Darunavir Interactions with Lipids for Developing pH-responsive Anti-HIV Drug Combination Nanoparticles, J Pharm Sci. 103 (2014) 2520–2529. doi:10.1002/jps.24046.Evaluation.

[12] J. Freeling, J. Koehn, C. Shu, J. Sun, R. Ho, Anti-HIV Drug-Combination Nanoparticles Enhance as Well as Triple-Drug Combination Levels in Cells Within Lymph Nodes and Blood in Primates, AIDS Res. Hum. Retrviruses. 31 (2015) 107–114. doi:10.1089/aid.2014.0210.

[13] J. Freeling, J. Koehn, C. Shu, J. Sun, R. Ho, Long-acting three-drug combination anti-HIV nanoparticles enhance drug exposure in primate plasma and cells within lymph nodes and blood, AIDS. 28 (2014) 2625–2631.

[14] S.N. Kudalkar, I. Ullah, N. Bertoletti, H.K. Mandl, J.A. Cisneros, J. Beloor, A.H. Chan, E. Quijano, W.M. Saltzman, W.L. Jorgensen, P. Kumar, K.S. Anderson, Structural and pharmacological evaluation of a novel non-nucleoside reverse transcriptase inhibitor as a promising long acting nanoformulation for treating HIV, Antiviral Res. 167 (2019) 110–116. doi:10.1016/j.antiviral.2019.04.010.

[15] S. Mandal, G. Kang, P. Kumar, W. Fan, Q. Li, C.J. Destache, Long-acting parenteral combination antiretroviral loaded nano-drug delivery system to treat chronic HIV-1 infection : A humanized mouse model study, Antiviral Res. 156 (2018) 85–91.

doi:10.1016/j.antiviral.2018.06.005.

[16] C. Trezza, S.L. Ford, W. Spreen, R. Pan, Formulation and pharmacology of long-acting cabotegravir, Curr Opin HIV AIDS. 10 (2015) 239–245. doi:10.1097/COH.0000000000000168.

[17] P.E. Williams, H.M. Crauwels, E.D. Basstanie, Formulation and pharmacology of long-acting rilpivirine, Curr. Opin. HIV AIDS. 10 (2015) 233–238. doi:10.1097/COH.0000000000000164.

[18] R.P. Bakshi, L.M. Tatham, A.C. Savage, A.K. Tripathi, G. Mlambo, M.M. Ippolito, E. Nenortas, S.P. Rannard, A. Owen, T.A. Shapiro, Long-acting injectable atovaquone nanomedicines for malaria prophylaxis, Nat. Commun. 9 (2018) 1–8. doi:10.1038/s41467-017-02603-z.

[19] Q. Li, L. Xie, D. Caridha, Q. Zeng, J. Zhang, N. Roncal, P. Zhang, C. Vuong, B. Potter, J. Sousa, S. Marcsisin, L. Read, M. Hickman, Long-Term Prophylaxis and Pharmacokinetic Evaluation of Intramuscular Nano- and Microparticle Decoquinate in Mice Infected with P . berghei Sporozoites, Malar. Res. Treat. (2016) 1–10.

[20] P. Narayanasamy, B.L. Switzer, B.E. Britigan, Prolonged-Acting, Multi-targeting Gallium Nanoparticles Potently Inhibit Growth of Both HIV and Mycobacteria in Co-infeccted Human Macrophages, Sci. Rep. 5 (2015) 1–7. doi:10.1038/srep08824.

[21] B.J. Edagwa, D. Guo, P. Puligujja, H. Chen, J. Mcmillan, X. Liu, H.E. Gendelman, P. Narayanasamy, Long-acting antituberculous therapeutic nanoparticles target macrophage endosomes, Res. Commun. 28 (2014) 1–12. doi:10.1096/fj.14-255786.

[22] A. Owen, S. Rannard, Strengths, weaknesses, opportunities and challenges for long acting injectable therapies: Insights for applications in HIV therapy, Adv. Drug Deliv.

Rev. 103 (2016) 144–156. doi:10.1016/j.addr.2016.02.003.

[23] S. Swindells, M. Siccardi, S.E. Barrett, D.B. Olsen, J.A. Grobler, A. Podany, E. Nuermberger, P. Kim, C. Barry, A. Owen, Long-acting formulations for the treatment of latent Tuberculosis infection: Opportunities and Challenges, Int J Tuberc Lung Dis. 22 (2018) 125–132. doi:10.5588/ijtld.17.0486.Long-Acting.

[24] Q. Mu, J. Yu, L.A. Mcconnachie, J.C. Kraft, Y. Gao, G.K. Gulati, R.J.Y. Ho, Translation of combination nanodrugs into nanomedicines: lessons learned and future outlook, J Drug Target. 26 (2018) 435–447. doi:10.1080/1061186X.2017.1419363.Translation.

[25] W.R. Spreen, D.A. Margolis, J.C. Pottage, Long-acting injectable antiretrovirals for HIV treatment and prevention, Curr. Opin. HIV AIDS. 8 (2013) 565–571. doi:10.1097/COH.0000000000000002.

[26] C.A. Lipinski, F. Lombardo, B. Dominy, P. Feeney, Experimental and computational approaches to estimate solubility and permeability in drug discovery and development settings, Adv. Drug Deliv. Rev. 23 (1997) 3–25.

[27] T. Oashi, A. Ringer, P. Raman, A.D. MacKrell, Automated selection of compounds with physicochemical properties to maximize bioavailability and druglikeness, J Chem Inf Model. 51 (2012) 148–158. doi:10.1021/ci100359a.Automated.

[28] B.C. Doak, F. Giordanetto, J. Kihlberg, Oral Druggable Space beyond the Rule of 5 : Insights from Drugs and Clinical Candidates, Chem. Biol. 21 (2014) 1115–1142. doi:10.1016/j.chembiol.2014.08.013.

[29] J.F. Remenar, Making the Leap from Daily Oral Dosing to Long-Acting Injectables : Lessons from the Antipsychotics, Mol. Pharm. 11 (2014) 1739–1749.

[30] I.M. Ibrahim, D. Soni, H.E. Gendelman, Synthesis and characterization of a long-acting emtricitabine prodrug nanoformulation, Int. J. Nanome. 14 (2019) 6231–6247.

[31] N. Smith, A.N. Bade, D. Soni, N. Gautam, Y. Alnouti, J. Herskovitz, I.M. Ibrahim, M.S. Wojtkiewicz, B. Laxmi, D. Shetty, J. Mcmillan, H.E. Gendelman, B. Edagwa, A long acting nanoformulated lamivudine ProTide, Biomaterials. 223 (2019) 1–11. doi:10.1016/j.biomaterials.2019.119476.

[32] C. Brasso, P. Rocca, Role of 3-monthly long-acting injectable paliperidone in the maintenance of schizophrenia, Neuropsychiatr. Dis. Treat. 13 (2017) 2767–2779.

[33] G.V.J. Klooster, E. Hoeben, H. Borghys, A. Looszova, M. Bouche, F. Van Velsen, L. Baert, Pharmacokinetics and Disposition of Rilpivirine (TMC278) Nanosuspension as a Long-Acting Injectable Antiretroviral Formulation □, Antimicrob. Agents Chemother. 54 (2010) 2042–2050. doi:10.1128/AAC.01529-09.

[34] K. Palm, P. Stenberg, K. Luthman, P. Artursson, Polar molecular surface properties predict the intestinal absorption of drugs in humans, Pharm. Res. 14 (1997) 568–571.

[35] L.Z. Benet, F. Broccatelli, T.I. Oprea, BDDCS Applied to Over 900 Drugs, AAPS J. 13 (2011) 519–546. doi:10.1208/s12248-011-9290-9.

[36] L.Z. Benet, C.M. Hosey, O. Ursu, T.I. Oprea, BDDCS, the Rule of 5 and Drugability, Adv Drug Deliv Rev. 101 (2016) 89–98. doi:10.1016/j.addr.2016.05.007.BDDCS.

[37] C.M.O. Driscoll, B.T. Griffin, Biopharmaceutical challenges associated with drugs with low aqueous solubility — The potential impact of lipid-based formulations ☆, Adv. Drug Deliv. Rev. 60 (2008) 617–624. doi:10.1016/j.addr.2007.10.012.

[38] M.R. Gigliobianco, C. Casadidio, R. Censi, P. Di MArtino, Nanocrystals of Poorly Soluble Drugs : Drug Bioavailability and Physicochemical Stability, Pharmaceutics. 10

(2018) 1–29. doi:10.3390/pharmaceutics10030134.

[39] J. Kraft, L. McConnachie, J. Koehn, L. Kinman, J. Sun, A. Collier, C. Collins, D. Shen, R. Ho, Mechanism-based pharmacokinetic (MBPK) models describe the complex plasma kinetics of three antiretrovirals delivered by a long-acting anti-HIV drug combination nanoparticle formulation, J. Control. Release. 275 (2018) 229–241. doi:10.1016/j.jconrel.2018.02.003.

[40] T. Zhou, H. Su, P. Dash, Z. Lin, B. Laxmi, D. Shetty, T. Kocher, A. Szlachetka, B. Lamberty, H.S. Fox, L. Poluektova, S. Gorantla, J. Mcmillan, N. Gautam, R.L. Mosley, Y. Alnouti, B. Edagwa, H.E. Gendelman, Creation of a nanoformulated cabotegravir prodrug with improved antiretroviral pro fi les, Biomaterials. 151 (2018) 53–65. doi:10.1016/j.biomaterials.2017.10.023.

[41] S.A. Hassounah, T. Mesplède, Where are we with injectables against HIV infection and what are the remaining challenges?", Expert Rev. Anti. Infect. Ther. 16 (2018) 143–152. doi:10.1080/14787210.2018.1430570.

[42] E. Ahire, S. Thakkar, M. Darshanwad, M. Misra, Parenteral nanosuspensions : a brief review from solubility enhancement to more novel and speci fi c applications, Acta Pharm. Sin. B. 8 (2018) 733–755. doi:10.1016/j.apsb.2018.07.011.

[43] L. Baert, G. Van, W. Dries, M. François, A. Wouters, E. Basstanie, K. Iterbeke, F. Stappers, P. Stevens, L. Schueller, P. Van Remoortere, G. Kraus, P. Wigerinck, J. Rosier, Development of a long-acting injectable formulation with nanoparticles of rilpivirine (TMC278) for HIV treatment, Eur. J. Pharm. Biopharm. 72 (2009) 502–508. doi:10.1016/j.ejpb.2009.03.006.

[44] R.J. Landovitz, S. Li, B.G. Id, H. Dawood, A.Y. Liu, M. Magnus, M.C. Hosseinipour, R. Panchia, L. Cottle, G. Chau, P. Richardson, M.A. Marzinke, C.W. Hendrix, S.

Eshleman, Y. Zhang, T. Elizabeth, J. Sugarman, R. Kofron, A. Adeyeye, D. Burns, A.R. Rinehart, D. Margolis, W.R. Spreen, M.S. Cohen, M. Mccauley, J.J.E. Id, Safety , tolerability , and pharmacokinetics of long-acting injectable cabotegravir in low-risk HIV-uninfected individuals : HPTN 077 , a phase 2a randomized controlled trial, PLOS Med. Med. 15 (2018) 1–22.

[45] J. Scallan, V. Huxley, R. Korthuis, The Lymphatic Vasculature, in: Capill. Fluid Exch. Regul. Funct. Pathol., 2010.

[46] A.A. Khan, J. Mudassir, N. Mohtar, Y. Darwis, Advanced drug delivery to the lymphatic system : lipid-based nanoformulations, Int. J. Nanomedicine. 8 (2013) 2733–2744.

[47] J.E. Moore, C.D. Bertram, Lymphatic System Flows, Annu Rev Fluid Mech. 50 (2018) 459–482. doi:10.1146/annurev-fluid-122316-045259.Lymphatic.

[48] M. Horiike, S. Iwami, M. Kodama, A. Sato, Y. Watanabe, M. Yasui, Lymph nodes harbor viral reservoirs that cause rebound of plasma viremia in SIV-infected macaques upon cessation of combined antiretroviral therapy, Virology. 423 (2012) 107–118. doi:10.1016/j.virol.2011.11.024.

[49] Y. Dimopoulos, E. Moysi, C. Petrovas, The Lymph Node in HIV Pathogenesis, Curr HIV/AIDS Rep. (2017). doi:10.1007/s11904-017-0359-7.

[50] A.R. Abell, M.J.S. Erea, B. Anxo, V. Marcos, Polyaminoacid Nanocapsules for Drug Delivery to the Lymphatic System : Effect of the Particle Size, Int. J. Pharm. 509 (2016) 107–117. doi:10.1016/j.ijpharm.2016.05.034.

[51] S. Aquaro, R. Calio, J. Balzarini, C. Bellocchi, E. Garaci, C. Federico, Macrophages and HIV infection : therapeutical approaches toward this strategic virus reservoir,

Antiviral Res. 55 (2002) 209–225.

[52] V. Schafer, H. von Briesen, R. Andreesen, A.-M. Steffan, C. Royer, S. Troster, J. Kreuter, H.R. Waigmann, Phagocytosis of Nanoparticles by Human Immunodeficiency Virus (HIV)-Infected Macrophages: A Possibility for Antiviral Drug Targeting, Pharm. Res. 9 (1992) 541–546.

[53] S.X. Jin, D.Z. Bi, J. Wang, Y.Z. Wang, H.G. Hu, Y.H. Deng, Pharmacokinetics and tissue distribution of zidovudine in rats following intravenous administration of zidovudine myristate loaded liposomes, Pharmazie. 60 (2005) 99–102.

[54] H. Dou, C.B. Grotepas, J.M. Mcmillan, C.J. Destache, J. Werling, J. Kipp, B. Rabinow, H.E. Gendelman, Macrophage delivery of nanoformulated antiretroviral drug to the brain in a murine model of neuroAIDS, J Immunol. 183 (2009) 661–669. doi:10.4049/jimmunol.0900274.Macrophage.

[55] A.L. Martinez-skinner, M.A. Araínga, P. Puligujja, D.L. Palandri, Cellular Responses and Tissue Depots for Nanoformulated Antiretroviral Therapy, PLoS One. 10 (2015) 1–19. doi:10.1371/journal.pone.0145966.

[56] L.M. Tatham, A.C. Savage, A. Dwyer, M. Siccardi, T. Scott, M. Vourvahis, A. Clark, S.P. Rannard, A. Owen, Towards a Maraviroc long-acting injectable nanoformulation, Eur. J. Pharm. Biopharm. 138 (2019) 92–98. doi:10.1016/j.ejpb.2018.04.009.

[57] B.L. Critchley, How Solid Drug Nanoparticles Can Tackle Drug Adherence Issues, (2018) 4–7. https://www.azonano.com/article.aspx?ArticleID=4974 (accessed April 11, 2020).

[58] S. Onoue, S. Yamada, H. Chan, Nanodrugs : pharmacokinetics and safety, Int. J. Nanomedicine. 9 (2014) 1025–1037.

[59] T.O. Mcdonald, M. Giardiello, P. Martin, M. Siccardi, N.J. Liptrott, D. Smith, P. Roberts, P. Curley, A. Schipani, S.H. Khoo, J. Long, A.J. Foster, S.P. Rannard, A. Owen, Antiretroviral Solid Drug Nanoparticles with Enhanced Oral Bioavailability : Production , Characterization , and In Vitro – In Vivo Correlation, Adv. Heal. Mater. 3 (2014) 400–411. doi:10.1002/adhm.201300280.

[60] M. Siccardi, P. Martin, D. Smith, P. Curley, T. Mcdonald, M. Giardiello, N. Liptrott, S. Rannard, A. Owen, Towards a rational design of solid drug nanoparticles with optimised pharmacological properties, J. Interdiscip. Nanomedicine. 1 (2016) 110–123. doi:10.1002/jin2.21.

[61] A.C. Savage, L.M. Tatham, M. Siccardi, T. Scott, M. Vourvahis, A. Clark, S.P. Rannard, A. Owen, Improving maraviroc oral bioavailability by formation of solid drug nanoparticles, Eur. J. Pharm. Biopharm. 138 (2020) 30–36. doi:10.1016/j.ejpb.2018.05.015.

[62] H.I. V London, V. Healthcare, S. Limited, N.D. Application, U.S. Food, HiiV Healthcare submits new drug application to US FDA for the first monthly, injectable, two-drug regimen of Cabotegravir and Rilpivirne for tretament of HIV, (2019). https://viivhealthcare.com/en-gb/media/press-releases/2019/april/viiv-healthcare-submits-new-drug-application-to-us-fda-for-the-first-monthly-injectable-two-drug-regimen-of-cabotegravir-and-rilpivirine-for-treatment-of-hiv (accessed April 11, 2020).

[63] P. Puligujja, S.S. Balkundi, L.M. Kendrick, H.M. Baldridge, J.R. Hilaire, A.N. Bade, P.K. Dash, G. Zhang, L.Y. Poluektova, S. Gorantla, X. Liu, T. Ying, Y. Feng, Y. Wang, D.S. Dimitrov, J.M. Mcmillan, H.E. Gendelman, Pharmacodynamics of long-acting folic acid-receptor targeted ritonavir-boosted atazanavir nanoformulations,

Biomaterials. 41 (2015) 141–150. doi:10.1016/j.biomaterials.2014.11.012.

[64] U. Roy, J. Mcmillan, Y. Alnouti, N. Gautum, N. Smith, S. Balkundi, P. Dash, S. Gorantla, A. Martinez-skinner, J. Meza, G. Kanmogne, S. Swindells, S.M. Cohen, R.L. Mosley, L. Poluektova, H.E. Gendelman, Pharmacodynamic and Antiretroviral Activities of Combination Nanoformulated Antiretrovirals in HIV-1 – Infected Human Peripheral Blood Lymphocyte – Reconstituted Mice, J. Infect. Dis. 206 (2012) 1577–1588. doi:10.1093/infdis/jis395.

[65] S. Choi, B.E. Britigan, P. Narayanasamy, Ga (III) Nanoparticles Inhibit Growth of Both TB and HIV and Release of IL-6 and IL-8 in Co-Infected Macrophages, Antimicrob. Agents Chemother. (2017). doi:10.1128/AAC.02505-16.

[66] B.M. Jucker, H. Alsaid, M. Rambo, S.C. Lenhard, B. Hoang, F. Xie, M.R. Groseclose, S. Castellino, V. Damian, G. Bowers, M. Gupta, Multimodal imaging approach to examine biodistribution kinetics of Cabotegravir (GSK1265744) long acting parenteral formulation in rat, J. Control. Release. 268 (2017) 102–112. doi:10.1016/j.jconrel.2017.10.017.

[67] M.G. Banoub, A.N. Bade, Z. Lin, D. Cobb, N. Gautam, B. Laxmi, D. Shetty, M. Wojtkiewicz, Y. Alnouti, J. Mcmillan, H.E. Gendelman, B. Edagwa, Synthesis and Characterization of Long-Acting Darunavir Prodrugs, Mol. Pharm. 17 (2020) 155–166. doi:10.1021/acs.molpharmaceut.9b00871.

[68] D. Guo, T. Zhou, M. Araínga, D. Palandri, N. Gautam, T. Bronich, Y. Alnouti, J. Mcmillan, B. Edagwa, H.E. Gendelman, Creation of a Long-Acting Nanoformulated 2',3'-Dideoxy-3'-Thiacytidine, J Acquir Immune Defic Syndr. 74 (2017) 75–83.

[69] Z. Lin, N. Gautam, Y. Alnouti, J. Mcmillan, A.N. Bade, H.E. Gendelman, B. Edagwa, ProTide generated long-acting abacavir nanoformulations, Chem. Commun. 54 (2018)

8371–8374. doi:10.1039/c8cc04708a.

[70] H.E.G. Brady Sillman, Aditya N. Bade, Prasanta K. Dash, Biju Bhargavan, Ted Kocher, Saumi Mathews, Hang Su, Georgette D. Kanmogne, Larisa Y. Pluektova, Santhi Gorantla, JoEllyn McMillan, Nagsen Gautam, Yazen Alnouti, Benson Edagwa, Creation of a long-acting nanoformulated dolutegravir, Nat. Commun. 9 (2018) 1–14. doi:10.1097/QAI.0000000000001170.

[71] J. Shen, D.J. Burgess, Accelerated in-vitro release testing methods for extended-release parenteral dosage forms, J. Pharm. Pharamcology. 64 (2012) 986–996. doi:10.1111/j.2042-7158.2012.01482.x.

[72] C. Hansch, J. Bjorkroth, A. Leo, Hydrophobicity and central nervous system agents: On the principle of minimal hydrophobicity in drug deisgn, J. Pharamceutical Sci. 76 (1987) 663–687.

[73] S. Mandal, M. Belshan, A. Holec, Y. Zhou, C. Destache, An Enhanced Emtricitabine-Loaded Long-Acting Nanoformulation for Prevention or Treatment of HIV Infection, Antimicrob. Agents Chemother. 61 (2017) 1–11.

[74] S. Mandal, P. Kumar, M. Belshan, C.J. Destache, A potential long-acting bictegravir loaded nano-drug delivery system for HIV-1 infection : A proof-of-concept study, Antiviral Res. 167 (2019) 83–88. doi:10.1016/j.antiviral.2019.04.007.

[75] S. Mandal, P.K. Prathipati, G. Kang, Y. Zhao, Z. Yuan, W. Fan, Q. Li, C. Destache, Tenofovir alafenamide and elvitegravir loaded nanoparticles for long-acting prevention of HIV-1 vaginal transmission, AIDS. 31 (2018) 469–476. doi:10.1097/QAD.0000000000001349.Tenofovir.

[76] S. Mandal, G. Kang, P. Kumar, Y. Zhou, W. Fan, Q. Li, C.J. Destache,

Nanoencapsulation introduces long-acting phenomenon to tenofovir alafenamide and emtricitabine drug combination : A comparative pre- exposure prophylaxis e ffi cacy study against HIV-1 vaginal transmission, J. Control. Release. 294 (2019) 216–225. doi:10.1016/j.jconrel.2018.12.027.

[77] P.K. Prathipati, S. Mandal, G. Pon, R. Vivekanandan, C.J. Destache, Pharmacokinetic and Tissue Distribution Profile of Long Acting Tenofovir Alafenamide and Elvitegravir Loaded Nanoparticles in Humanized Mice Model, Pharm Res. 34 (2017) 2749–2755. doi:10.1007/s11095-017-2255-7.

[78] What is Pre Exposure Prophylaxis (PrEP), (n.d.). https://www.avert.org/hiv-transmission-prevention/prep (accessed April 13, 2020).

[79] M. Markowitz, I. Frank, R.M. Grant, K.H. Mayer, R. Elion, D. Goldstein, C. Fisher, M.E. Sobieszczyk, A.R. Rinehart, K.Y. Smith, W.R. Spreen, Safety and tolerability of long-acting cabotegravir injections in HIV-uninfected men (ECLAIR): a multicentre , double-blind , randomised , placebo-controlled , phase 2a trial, Lancet HIV. (2017) 1–10. doi:10.1016/S2352-3018(17)30068-1.

[80] A. Attama, M. Momoh, P. Builders, Lipid Nanoparticulate Drug Delivery Systems: A Revolution in Dosage Form Design and Development, in: Recent Adv. Nov. Drug Carr. Syst., 2012: pp. 107–140.

[81] H. Raina, S. Kaur, A.B. Jindal, Development of efavirenz loaded solid lipid nanoparticles: Risk assessment, quality-by-design (QbD) based optimisation and physicochemical characterisation, J. Drug Deliv. Sci. Technol. 39 (2017) 180–191. doi:10.1016/j.jddst.2017.02.013.

[82] D.H. Surve, A.B. Jindal, Development and validation of reverse-phase high-performance liquid chromatographic (RP-HPLC) method for quantification of

Efavirenz in Efavirenz-Enfuvirtide co-loaded polymer-lipid hybrid nanoparticles, J. Pharm. Biomed. Anal. 175 (2019) 112765. doi:10.1016/j.jpba.2019.07.013.

[83] M.W. Kim, S. Kwon, J.H. Choi, A. Lee, A Promising Biocompatible Platform : Lipid-Based and Bio-Inspired Smart Drug Delivery Systems for Cancer Therapy, Int. J. Mol. Sci. 19 (2018) 1–20. doi:10.3390/ijms19123859.

[84] A. Laine, J. Gravier, M. Henry, L. Sancey, J. Béjaud, E. Pancani, M. Wiber, I. Texier, J. Coll, J. Benoit, C. Passirani, Conventional versus stealth lipid nanoparticles: Formulation and in vivo fate prediction through FRET monitoring, J. Control. Release. 188 (2014) 1–8. doi:10.1016/j.jconrel.2014.05.042.

[85] A.B. Jindal, S.S. Bachhav, P. V. Devarajan, In situ hybrid nano drug delivery system (IHN-DDS) of antiretroviral drug for simultaneous targeting to multiple viral reservoirs: An in vivo proof of concept, Int. J. Pharm. 521 (2017) 196–203. doi:10.1016/j.ijpharm.2017.02.024.

[86] P.K. Dash, H.E. Gendelman, U. Roy, S. Balkundi, R.L. Mosley, H.A. Gelbard, J. Mcmillan, S. Gorantla, L.Y. Poluektova, Long-acting NanoART Elicits Potent Antiretroviral and Neuroprotective Responses in HIV-1 Infected Humanized Mice, AIDS. 26 (2014) 2135–2144. doi:10.1097/QAD.0b013e328357f5ad.Long-acting.

[87] J. McMillan, A. Sclachetka, L. Slack, B. Sillman, B. Lamberty, B. Morsey, S. Callen, N. Gautam, Y. Alnouti, B. Edagwa, H. Gendelman, H. Fox, Pharmacokinetics of a Long-Acting Nanoformulated Dolutegravir Prodrug in Rhesus Macaques, Antimicrob. Agents Chemother. 62 (2018) 1–5.

[88] J.J. Hobson, A. Al-khouja, P. Curley, D. Meyers, C. Flexner, M. Siccardi, A. Owen, C.F. Meyers, S.P. Rannard, Semi-solid prodrug nanoparticles for long-acting delivery of water-soluble antiretroviral drugs within combination HIV therapies, Nat. Commun.

10 (2019) 1–10. doi:10.1038/s41467-019-09354-z.

[89] S.N. Kudalkar, J. Beloor, E. Quijano, K.A. Spasov, W. Lee, J.A. Cisneros, From in silico hit to long-acting late-stage preclinical candidate to combat HIV-1 infection, PNAS PLUS. (2017) 1–10. doi:10.1073/pnas.1717932115.

[90] R. Paliwal, R.J. Babu, S. Palakurthi, Nanomedicine Scale-up Technologies : Feasibilities and Challenges, AAPS PharmSciTech. 15 (2014) 1527–1534. doi:10.1208/s12249-014-0177-9.

[91] H.E. Gendelman, J. Mcmillan, A.N. Bade, B. Edagwa, B.D. Kevadiya, The Promise of Long-Acting Antiretroviral Therapies : From Need to Manufacture, Trends Microbiol. 27 (2019) 593–606. doi:10.1016/j.tim.2019.02.009.

[92] N. Desai, Challenges in Development of Nanoparticle-Based Therapeutics, AAPS JournalAAPS. 14 (2012) 282–295. doi:10.1208/s12248-012-9339-4.

[93] M. Barnhart, Long-Acting Tretament and Prevention: Closer to the Threshold, Glob. Heal. Sci. Pract. 5 (2017) 182–187.

[94] W.R. Spreen, D.A. Margolis, J.C. Pottage, Long-acting injectable antiretrovirals for HIV treatment and prevention, Curr Opin HIV AIDS. 8 (2013) 565–571. doi:10.1097/COH.0000000000000002.

[95] P.K. Dash, R. Kaminski, R. Bella, H. Su, S. Mathews, T.M. Ahooyi, C. Chen, P. Mancuso, R. Sariyer, P. Ferrante, M. Donadoni, J.A. Robinson, B. Sillman, Z. Lin, J.R. Hilaire, M. Banoub, M. Elango, N. Gautam, R.L. Mosley, L.Y. Poluektova, J. Mcmillan, A.N. Bade, S. Gorantla, I.K. Sariyer, T.H. Burdo, W. Young, S. Amini, J. Gordon, J.M. Jacobson, B. Edagwa, K. Khalili, H.E. Gendelman, Sequential LASER ART and CRISPR Treatments Mice, Nat. Commun. 10 (2019) 1–20.

doi:10.1038/s41467-019-10366-y.

[96] D.H. Surve, A.B. Jindal, Recent advances in long-acting nanoformulations for delivery of antiretroviral drugs, J. Control. Release. 324 (2020) 379–404. doi:10.1016/j.jconrel.2020.05.022.

[97] African animal trypanosomosis, (n.d.). http://www.fao.org/3/x0413e/X0413E05.htm (accessed August 4, 2020).

[98] TRUVADA®, (n.d.). https://www.accessdata.fda.gov/drugsatfda_docs/label/2005/21752s002lbl.pdf (accessed August 29, 2020).

[99] J. Labonte, J. Lebbos, P. Kirkpatrick, Enfuvirtide, Nat. Rev. Drug Discov. 2 (2003) 345–346. doi:10.1038/nrd1091.

[100] P.L. Vernazza, P. Schmid, Antiviral drugs, Elsevier B.V., 2005. doi:10.1016/S0378-6080(05)80451-9.

[101] H. Hardy, P. Skolnik, Enfuvirtide , a New Fusion Inhibitor for Therapy of Human Immunodeficiency Virus Infection, Pharmacotherapy. 24 (2004) 198–211.

[102] I.H. Patel, X. Zhang, K. Nieforth, M. Salgo, N. Buss, Pharmacokinetics, pharmacodynamics and drug interaction potential of enfuvirtide, Clin. Pharmacokinet. 44 (2005) 175–186. doi:10.2165/00003088-200544020-00003.

[103] D.N. Kapoor, O.P. Katare, S. Dhawan, In situ forming implant for controlled delivery of an anti-HIV fusion inhibitor, Int. J. Pharm. 426 (2012) 132–143. doi:10.1016/j.ijpharm.2012.01.005.

[104] X. Ding, X. Zhang, Chong, Huihui, Y. Zhu, H. Wei, J. He, X. Wang, Y. He, Enfuvirtide (T20)-based Lipopeptide Is a Potent HIV-1 Cell Fusion Inhibitor:

Implication for Viral Entry and Inhibition, J. Virol. (2017). doi:10.1128/JVI.00831-17.

[105] Isometamidium chloride, (n.d.). https://pubchem.ncbi.nlm.nih.gov/compound/Isometamidium-chloride (accessed August 1, 2020).

[106] L.D.. Kinabo, J.A.. Bogan, The pharmacology of isometamidium, J.Vet. Pharmcol. Ther. 11 (1988) 233–245.

[107] Isometamidium, (n.d.). http://www.inchem.org/documents/jecfa/jecmono/v25je10.htm (accessed August 1, 2020).

[108] G.A. Murilla, R.E. Mdachi, W.. Karanja, Pharmacokinetics, bioavailability and tissue residues of [14C] isometamidium in non-infected and Trypanosoma congolense-infected Boran cattle, Acta Trop. 61 (1996) 277–292.

[109] S. Singh, M. Chopra, N. Dilbaghi, B.K. Manuja, S. Kumar, R. Kumar, N.S. Rathore, S.C. Yadav, A. Manuja, Synthesis and evaluation of isometamidium-alginate nanoparticles on equine mononuclear and red blood cells, Int. J. Biol. Macromol. 92 (2016) 788–794. doi:10.1016/j.ijbiomac.2016.07.084.